Previous Page

(1997).
[7.52] M. Steube, K. Reimann, D. Fröhlich, and S. J. Clarke, *Appl. Phys. Lett.* **71**, 948 (1997).
[7.53] L. Eckey, A. Hoffmann, P. Thurian, I. Broser, B. K. Meyer, and K. Hiramatsu, *Mat. Res. Soc. Symp. Proc.* **482**, 555 (1998).

10.8 ELECTRONIC DEFORMATION POTENTIAL

10.8.1 Intravalley Deformation Potential: Γ Point

• Conduction band

Table 10.8.1 *Γ-conduction-band deformation potentials D_1 and D_2 for α-GaN.*

Deformation potential (eV)		Comment
D_1	D_2	
−9.47	−7.17	Calc. [8.1]

[8.1] J. A. Majewski, M. Städele, and P. Vogl, *Mat. Res. Soc. Symp. Proc.* **449**, 887 (1997).

• Valence band

Table 10.8.2 *Theoretical Γ-valence-band deformation potentials C_i's for α-GaN.*

Deformation potential (eV)								Ref.
C_1	D_1–C_1	C_2	D_2–C_2	C_3	C_4	C_5	C_6	
−15.3		−12.4		3.0	−1.5	−2.0	−3.7	[8.2]
				5.7	−2.85			[8.3]
				6.26	−3.29			[8.4]
	−6.11		−9.62	5.76	−3.04			[8.5]
−20.0		−14.2		5.80	−3.25	−2.85		[8.6]

[8.2] M. Suzuki and T. Uenoyama, *Jpn. J. Appl. Phys.* **35**, L953 (1996).
[8.3] K. Kim, W. R. L. Lambrecht, B. Segall, and M. van Schilfgaarde, *Phys. Rev. B* **56**, 7363 (1997).
[8.4] J. A. Majewski, M. Städele, and P. Vogl, *Mat. Res. Soc. Symp. Proc.* **449**, 887 (1997).
[8.5] W. W. Chow, A. F. Wright, A. Girndt, F. Jahnke, and S. W. Koch, *Mat. Res. Soc. Symp. Proc.* **468**, 487 (1997).
[8.6] K. Shimada, T. Sota, and K. Suzuki, *Mat. Res. Soc. Symp. Proc.* **482**, 869 (1998).

Table 10.8.3 *Experimental Γ-valence-band deformation potentials C_i's for α-GaN.*

Deformation potential (eV)								Ref.
C_1	D_1–C_1	C_2	D_2–C_2	C_3	C_4	C_5	C_6	
				5.73	−2.86			[8.7]
	− 8.16		− 8.16	1.44	− 0.72			[8.8]
				8.82	−4.41			[8.9]
				8.82	−4.41			[8.10]
	−5.32		−10.23	4.91	−2.45			[8.11]
	−6.5		−11.8	5.3	−2.7			[8.12]

Table 10.8.3 *Continued.*

Deformation potential (eV)								Ref.
C_1	D_1–C_1	C_2	D_2–C_2	C_3	C_4	C_5	C_6	
						–2.4		[8.13]
				7.2	–3.6			[8.14]
–41.4	–3.1	–33.3	–11.2	8.2	–4.1	–4.7		[8.15]

[8.7] S. Chichibu, A. Shikanai, T. Azuhata, T. Sota, A. Kuramata, K. Horino, and S. Nakamura, *Appl. Phys. Lett.* **68**, 3766 (1996).
[8.8] M. Tchounkeu, O. Briot, B. Gil, J. P. Alexis, and R.-L. Aulombard, *J. Appl. Phys.* **80**, 5352 (1996).
[8.9] A. Shikanai, T. Azuhata, T. Sota, S. Chichibu, A. Kuramata, K. Horino, and S. Nakamura, *J. Appl. Phys.* **81**, 417 (1997).
[8.10] S. Chichibu, T. Azuhata, T. Sota, H. Amano, and I. Akasaki, *Appl. Phys. Lett.* **70**, 2085 (1997).
[8.11] B. Gil and A. Alemu, *Phys. Rev. B* **56**, 12446 (1997).
[8.12] W. Shan, A. J. Fischer, S. J. Hwang, B. D. Little, R. J. Hauenstein, X. C. Xie, J. J. Song, D. S. Kim, B. Goldenberg, R. Horning, S. Krishnankutty, W. G. Perry, M. D. Bremser, and R. F. Davis, *J. Appl. Phys.* **83**, 455 (1998).
[8.13] A. Alemu, B. Gil, M. Julier, and S. Nakamura, *Phys. Rev. B* **57**, 3761 (1998).
[8.14] A. A. Yamaguchi, Y. Mochizuki, H. Sunakawa, and A. Usui, *J. Appl. Phys.* **83**, 4542 (1998).
[8.15] S. Ghosh, P. Waltereit, O. Brandt, H. T. Grahn, and K. H. Ploog, *Phys. Rev. B* **65**, 75202 (2002).

• **E_0 gap**

Table 10.8.4 *Hydrostatic deformation potential a_0^{Γ} for the $E_{0\alpha}$ (α=A, B, or C) gap of α-GaN.*

a_0^{Γ} (eV)	Technique
–9.2±1.2	Photoluminescence [8.16]
–8.8±0.9	Photoluminescence, Reflectance [8.17]
–8.3	Estimated*
–8.8	Mean value

[8.16] W. Shan, T. J. Schmidt, R. J. Hauenstein, J. J. Song, and B. Goldenberg, *Appl. Phys. Lett.* **66**, 3492 (1995).
[8.17] B. J. Skromme, *Mater. Sci. Eng. B* **50**, 117 (1997).
*From a value of pressure coefficient $dE_{0\alpha}/dp$=4.3×10^{-2} eV/GPa and bulk modulus of B_u=192 GPa.

10.8.2 Intravalley Deformation Potential: High-Symmetry Points

No detailed data are available for α-GaN.

10.8.3 Intervalley Deformation Potential

• **Absolute value**

Table 10.8.5 *Intervalley deformation potential D_{ij}, for electrons in α-GaN.*

D_{ij} (eV/Å)		Ref.
Equivalent intervalley	Nonequivalent intervalley	
10	10	[8.18]
10	10	[8.19]
10	10	[8.20]
5	10	[8.21]

[8.18] U. V. Bhapkar and M. S. Shur, *J. Appl. Phys.* **82**, 1649 (1997).
[8.19] S. K. O'Leary, B. E. Foutz, M. S. Shur, U. V. Bhapkar, and L. F. Eastman, *J. Appl. Phys.* **83**, 826 (1998).
[8.20] B. E. Foutz, S. K. O'Leary, M. S. Shur, and L. F. Eastman, *J. Appl. Phys.* **85**, 7727 (1999).
[8.21] T. Li, R. P. Joshi, and C. Fazi, *J. Appl. Phys.* **88**, 829 (2000).

10.9 ELECTRON AFFINITY AND SCHOTTKY BARRIER HEIGHT

10.9.1 Electron Affinity

Table 10.9.1 *Electron affinity χ_s for α-GaN.*

χ_s (eV)	Comment
2.1–4.1	*n*-type and intrinsic GaN [9.1]
3.2±0.2	Sputter-cleaned GaN(0001) [9.2]
3.3±0.3	CVD-grown on 6H-SiC [9.3]
3.5±0.1	MOCVD-grown GaN(0001) [9.4]
3.1±0.2	MOCVD-grown GaN(0001) [9.5]
3.3±0.3	Recommended value

[9.1] J. I. Pankove and H. Schade, *Appl. Phys. Lett.* **25**, 53 (1974).
[9.2] V. M. Bermudez, *J. Appl. Phys.* **80**, 1190 (1996).
[9.3] M. C. Benjamin, M. D. Bremser, T. W. Weeks, Jr., S. W. King, R. F. Davis, and R. J. Nemanich, *J. Cryst. Growth* **104/105**, 455 (1996).
[9.4] C. I. Wu and A. Kahn, *J. Vac. Sci. Technol. B* **16**, 2218 (1998).
[9.5] S. P. Grabowski, M. Schneider, H. Nienhaus, W. Mönch, R. Dimitrov, O. Ambacher, and M. Stutzmann, *Appl. Phys. Lett.* **78**, 2503 (2001).

10.9.2 Schottky Barrier Height

Table 10.9.2 *Summary of the Schottky barrier height ϕ_n for metal/n-GaN contacts at T=300 K.*

Metal	Metal work function (eV)*	ϕ_n (eV)	Ref.
Pb	4.25	0.73	[9.6]
Ti	4.33	0.2–0.8	[9.6], [9.7]
Cr	4.5	0.52–0.57	[9.6]
Ag	4.63	0.54–1.61	[9.6], [9.7]
Re	4.72	0.82–1.06	[9.6]
Cu	4.76	0.77–1.41	[9.6], [9.8]
Co	5.0	0.90–0.93	[9.6]
Ni	5.20	0.56–1.18	[9.6], [9.7], [9.9]
Au	5.38	0.84–1.2	[9.6], [9.10]
Pd	5.41	0.90–1.52	[9.6]
Pt	5.55	0.88–1.57	[9.6], [9.11], [9.12]
RuO_2		0.90–1.04	[9.13]

[9.6] See, S. E. Mohney, in *Properties, Processing and Applications of Gallium Nitride and Related Semiconductors*, EMIS Datareviews Series No. 23, edited by J. H. Edgar, S. Strite, I. Akasaki, H. Amano, and C. Wetzel (INSPEC, London, 1999), p. 496.

[9.7] S. Arulkumaran, T. Egawa, G.-Y. Zhao, H. Ishikawa, T. Jimbo, and M. Umeno, *Jpn. J. Appl. Phys.* **39**, L351 (2000).
[9.8] W. C. Lai, M. Yokoyama, C. Y. Chang, J. D. Guo, J. S. Tsang, S. H. Chan, and S. M. Sze, *Mat. Res. Soc. Symp. Proc.* **572**, 523 (1999).
[9.9] K. Shiojima, J. M. Woodall, C. J. Eiting, P. A. Grudowski, and R. D. Dupuis, *J. Vac. Sci. Technol. B* **17**, 2030 (1999).
[9.10] S. K. Noh and P. Bhattacharya, *Appl. Phys. Lett.* **78**, 3642 (2001).
[9.11] Q. Z. Liu, L. S. Yu, K. V. Smith, F. Deng, C. W. Tu, P. M. Asbeck, E. T. Yu, and S. S. Lau, *Electrochem. Soc. Proc.* **97-34**, 11 (1997).
[9.12] J. M. DeLucca, S. E. Mohney, F. D. Auret, and S. A. Goodman, *J. Appl. Phys.* **88**, 2593 (2000).
[9.13] S.-H. Lee, J.-K. Chun, J.-J. Hur, J.-S. Lee, G.-H. Rue, Y.-H. Bae, S.-H. Hahm,Y.-H. Lee, and J.-H. Lee, *IEEE Electron. Dev. Lett.* **21**, 261 (2000).
*Taken from H. P. R. Frederikse [in *CRC Handbook of Chemistry and Physics*, 78th Edition, edited by D. R. Lide (CRC Press, Boca Raton, 1997), p. 12-115].

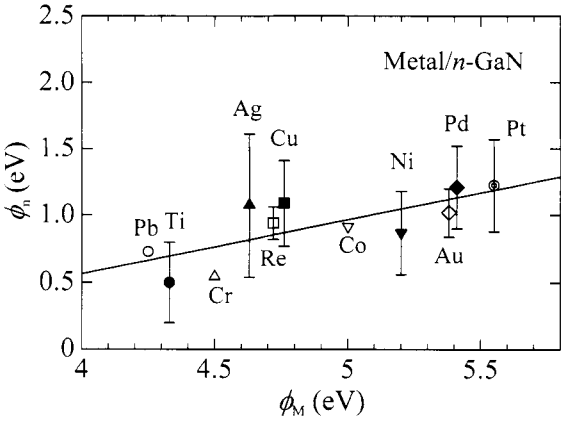

Fig. 10.9.1 Schottky barrier height ϕ_n versus metal work function ϕ_M observed for metal/*n*-GaN contacts. Values of the metal work function were taken from H. P. R. Frederikse [in *CRC Handbook of Chemistry and Physics*, 78th Edition, edited by D. R. Lide (CRC Press, Boca Raton, 1997), p. 12-115]. The solid line represents the least-squares-fit result with ϕ_n=0.40ϕ_M–1.05 (ϕ_M and ϕ_n in eV).

Table 10.9.3 *Summary of the Schottky barrier height ϕ_p for metal/p-GaN contacts.*

Metal	Metal work function (eV)*	ϕ_p (eV)	Ref.
Ti	4.33	0.65	[9.14]
Ni	5.20	0.50	[9.14]
		2.4	[9.15]
		2.68–2.87	[9.16]
Au	5.38	0.57	[9.14]
		2.48	[9.17]
Pt	5.55	0.50	[9.14]
Pt/Au		0.49	[9.18]
Ni/Au		0.49–0.58	[9.19]

[9.14] T. Mori, T. Kozawa, T. Ohwaki, Y. Taga, S. Nagai, S. Yamasaki, S. Asami, N. Shibata, and M. Koike, *Appl. Phys. Lett.* **69**, 3537 (1996).
[9.15] K. Shiojima, T. Sugahara, and S. Sakai, *Appl. Phys. Lett.* **74**, 1936 (1999).
[9.16] L. S. Yu, D. Qiao, L. Jia, S. S. Lau, Y. Qi, and K. M. Lau, *Appl. Phys. Lett.* **79**, 4536 (2001).
[9.17] N. I. Kuznetsov, E. V. Kalinina, V. A. Soloviev, and V. A. Dmitriev, *Mat. Res. Soc. Symp. Proc.* **395**, 837 (1996).
[9.18] X. A. Cao, S. J. Pearton, G. Dang, A. P. Zhang, F. Ren, and J. M. Van Hove, *Appl. Phys. Lett.* **75**, 4130 (1999).
[9.19] D. L. Hibbard, R. W. Chuang, Y. S. Zhao, C. L. Jensen, H. P. Lee, Z. J. Dong, R. Shin, and M. Bremser, *J. Electron. Mater.* **29**, 291 (2000).
*Taken from H. P. R. Frederikse [in *CRC Handbook of Chemistry and Physics*, 78th Edition, edited by D. R. Lide (CRC Press, Boca Raton, 1997), p. 12-115].

• **Breakdown voltage**

Table 10.9.4 *Breakdown field E_{BR} in α-GaN.*

E_{BR} (V/cm)	Ref.
2.6×10^6	[9.20]
3.3×10^6	[9.21]

[9.20] See, Yu. A. Goldberg, *Semicond. Sci. Technol.* **14**, R41 (1999).
[9.21] See, T. P. Chow, V. Khemka, J. Fedison, N. Ramungul, K. Matocha, Y. Tang, and R. J. Gutmann, *Solid-State Electron.* **44**, 277 (2000).

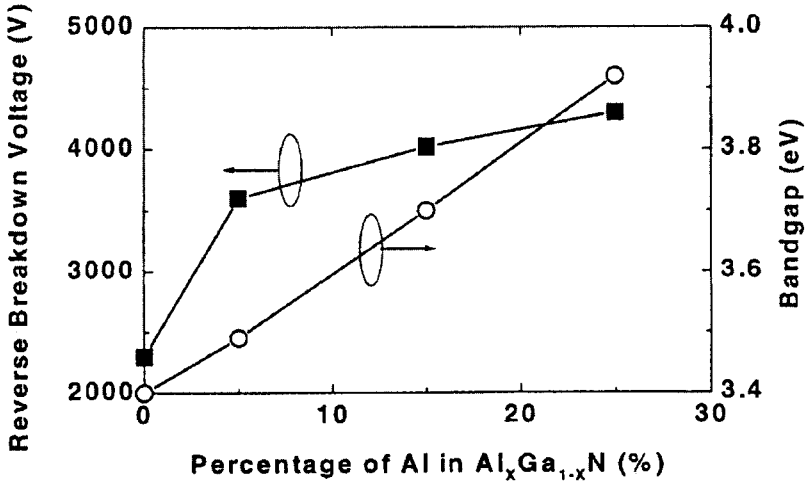

Figure 10.9.2 Variation of reverse breakdown voltage in $Al_xGa_{1-x}N$ lateral Schottky rectifiers without edge termination as a function of Al concentration x. The band gap as a function of x for $Al_xGa_{1-x}N$ is also shown. [From A. P. Zhang, G. Dang, F. Ren, J. Han, A. Y. Polyakov, N. B. Smirnov, A. V. Govorkov, J. M. Redwing, X. A. Cao, and S. J. Pearton, *Appl. Phys. Lett.* **76**, 1767 (2000).]

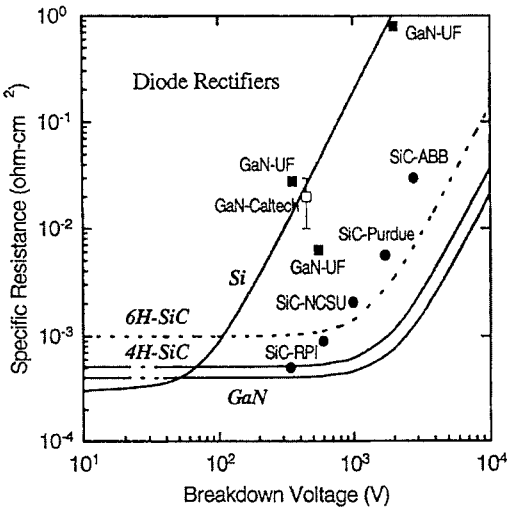

Figure 10.9.3 Specific on-resistance versus blocking voltage for GaN Schottky diode rectifiers, together with those for 4H-SiC and 6H-SiC Schottky diode rectifiers. The performance limits of GaN, SiC, and Si devices are also shown by the solid lines. [From C. T. Dang, A. P. Zhang, F. Ren, X. A. Cao, S. J. Pearton, H. Cho, J. Han, J.-I. Chyi, C.-M. Lee, C.-C. Chuo, S. N. G. Chu, and R. G. Wilson, *IEEE Trans. Electron Dev.* **47**, 692 (2000).]

10.10 OPTICAL PROPERTIES

10.10.1 Summary of Optical Dispersion Relations

• $\varepsilon(E)$ and $n^*(E)$ spectra

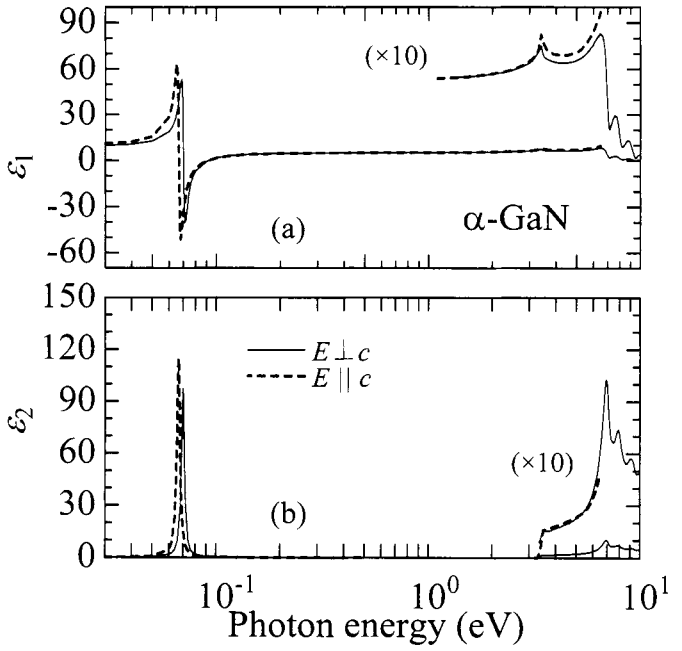

Fig. 10.10.1 Complex dielectric-constant spectra [$\varepsilon(E)=\varepsilon_1(E)+i\varepsilon_2(E)$] for α-GaN at 300 K. The numerical data are taken from tabulation given below.

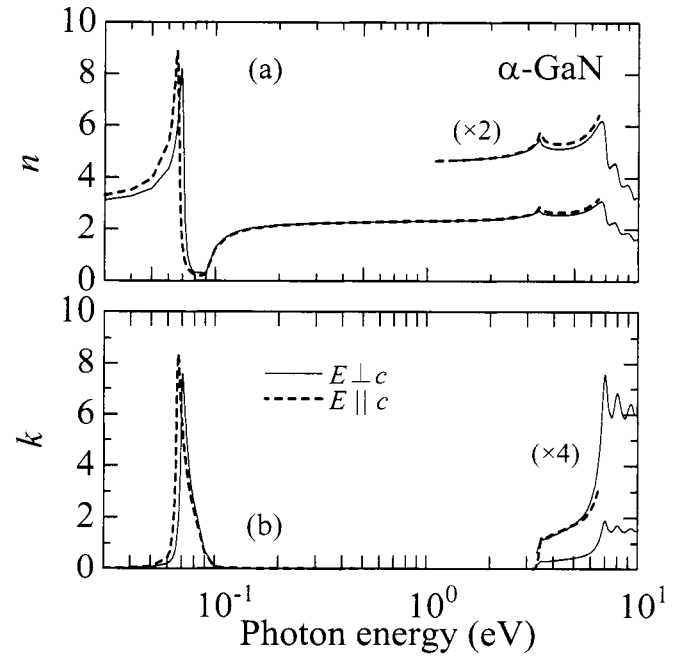

Fig. 10.10.2 (a) Complex refractive-index spectra [$n^*(E)=n(E)+ik(E)$] for α-GaN at 300 K. The numerical data are taken from tabulation given below.

• $\alpha(E)$ and $R(E)$ spectra

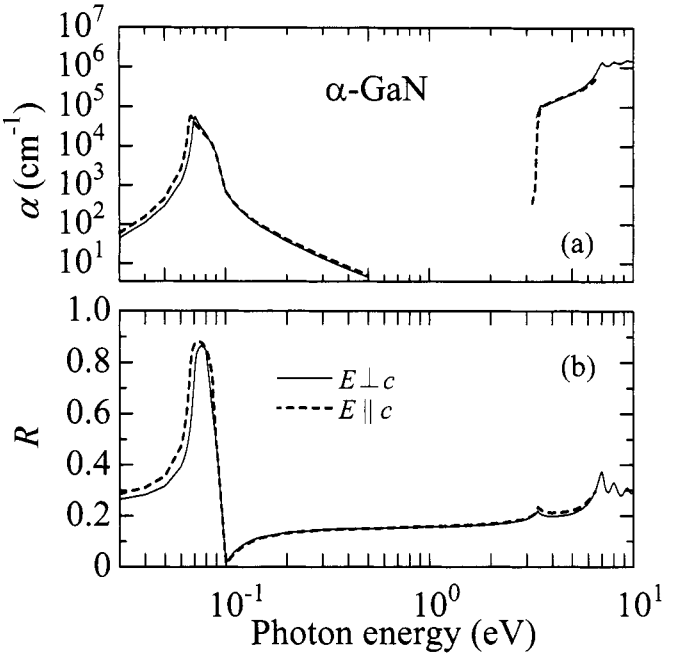

Fig. 10.10.3 (a) Absorption [$\alpha(E)$] and (b) normal-incidence reflectivity spectra [$R(E)$] for α-GaN at 300 K. The numerical data are taken from tabulation given below.

Table 10.10.1 *Optical constants of α-GaN for* $\boldsymbol{E}\perp c$ *at 300 K.**

eV	ε_1	ε_2	n	k	α (cm^{-1})	R
0.01	8.977	0.021	2.996	0.0035	3.54E+00	0.250
0.02	9.228	0.048	3.038	0.0078	1.59E+01	0.255
0.03	9.730	0.090	3.119	0.014	4.41E+01	0.265
0.04	10.69	0.177	3.269	0.027	1.10E+02	0.283
0.05	12.72	0.417	3.568	0.058	2.96E+02	0.316
0.06	18.91	1.680	4.352	0.193	1.17E+03	0.393
0.062	21.91	2.603	4.689	0.278	1.74E+03	0.422
0.064	26.69	4.534	5.185	0.437	2.84E+03	0.461
0.066	35.20	9.621	5.987	0.803	5.38E+03	0.516
0.068	50.85	29.50	7.404	1.992	1.37E+04	0.603
0.069	53.06	61.35	8.191	3.745	2.62E+04	0.667
0.0695	39.02	84.43	8.125	5.196	3.66E+04	0.705
0.07	7.517	97.22	7.247	6.708	4.76E+04	0.743
0.07025	-10.24	94.41	6.508	7.253	5.17E+04	0.761
0.0705	-24.93	86.03	5.685	7.567	5.41E+04	0.777
0.071	-40.31	63.06	4.155	7.588	5.46E+04	0.802
0.072	-38.93	30.29	2.280	6.642	4.85E+04	0.834
0.074	-23.17	9.789	0.996	4.916	3.69E+04	0.858
0.076	-14.55	4.591	0.594	3.861	2.97E+04	0.864
0.078	-9.721	2.629	0.418	3.146	2.49E+04	0.860
0.08	-6.692	1.695	0.325	2.607	2.11E+04	0.848
0.09	-0.447	0.424	0.291	0.729	6.65E+03	0.471
0.1	1.648	0.186	1.286	0.072	7.32E+02	0.017
0.11	2.682	0.103	1.638	0.031	3.49E+02	0.059

Table 10.10.1 *Continued.*

eV	ε_1	ε_2	n	k	α (cm^{-1})	R
0.12	3.291	0.064	1.814	0.018	2.16E+02	0.084
0.13	3.688	0.044	1.921	0.011	1.50E+02	0.099
0.14	3.966	0.031	1.991	0.0079	1.12E+02	0.110
0.15	4.169	0.023	2.042	0.0057	8.72E+01	0.117
0.2	4.683	0.0079	2.164	0.0018	3.68E+01	0.135
0.3	4.987	0.0020	2.233	0.00045	1.36E+01	0.145
0.4	5.083	0.00080	2.255	0.00018	7.23E+00	0.149
0.5	5.126	0.00040	2.264	0.000089	4.51E+00	0.150
1.3	5.459		2.336			0.160
1.4	5.477		2.340			0.161
1.5	5.503		2.346			0.162
1.6	5.529		2.351			0.163
1.7	5.564		2.359			0.164
1.8	5.591		2.365			0.164
1.9	5.644		2.376			0.166
2	5.680		2.383			0.167
2.1	5.724		2.393			0.168
2.2	5.751		2.398			0.169
2.3	5.796		2.408			0.171
2.4	5.850		2.419			0.172
2.5	5.932		2.436			0.175
2.6	6.014		2.452			0.177
2.7	6.106		2.471			0.180
2.8	6.208		2.492			0.182
2.9	6.302		2.510			0.185
3	6.405		2.531			0.188
3.1	6.577		2.565			0.193
3.2	6.848		2.617			0.200
3.3	7.155		2.675			0.208
3.35	7.300	0.889	2.707	0.164	5.57E+04	0.214
3.40	7.500	1.129	2.746	0.206	7.09E+04	0.220
3.45	7.059	1.404	2.670	0.263	9.20E+04	0.211
3.50	6.831	1.631	2.632	0.310	1.10E+05	0.208
3.55	6.747	1.596	2.615	0.305	1.10E+05	0.205
3.60	6.677	1.534	2.601	0.295	1.08E+05	0.203
3.65	6.622	1.531	2.590	0.296	1.09E+05	0.202
3.70	6.581	1.533	2.582	0.297	1.11E+05	0.201
3.75	6.549	1.546	2.577	0.300	1.14E+05	0.200
3.80	6.521	1.558	2.572	0.303	1.17E+05	0.199
3.85	6.497	1.602	2.568	0.312	1.22E+05	0.199
3.90	6.478	1.643	2.565	0.320	1.27E+05	0.199
3.95	6.455	1.670	2.561	0.326	1.31E+05	0.199
4.00	6.442	1.683	2.559	0.329	1.33E+05	0.199
4.05	6.427	1.705	2.557	0.333	1.37E+05	0.199

Table 10.10.1 *Continued.*

eV	ε_1	ε_2	n	k	α (cm^{-1})	R
4.10	6.416	1.744	2.556	0.341	1.42E+05	0.199
4.15	6.416	1.760	2.556	0.344	1.45E+05	0.199
4.20	6.409	1.772	2.555	0.347	1.48E+05	0.199
4.25	6.407	1.802	2.556	0.353	1.52E+05	0.199
4.30	6.403	1.842	2.556	0.360	1.57E+05	0.200
4.35	6.399	1.865	2.556	0.365	1.61E+05	0.200
4.40	6.401	1.890	2.557	0.370	1.65E+05	0.200
4.45	6.411	1.915	2.559	0.374	1.69E+05	0.201
4.50	6.425	1.936	2.563	0.378	1.72E+05	0.201
4.55	6.426	1.978	2.564	0.386	1.78E+05	0.202
4.60	6.438	1.986	2.567	0.387	1.80E+05	0.202
4.65	6.454	1.990	2.570	0.387	1.83E+05	0.203
4.70	6.459	2.044	2.572	0.397	1.89E+05	0.204
4.75	6.472	2.089	2.576	0.405	1.95E+05	0.204
4.80	6.487	2.120	2.580	0.411	2.00E+05	0.205
4.85	6.502	2.148	2.584	0.416	2.04E+05	0.206
4.90	6.521	2.186	2.588	0.422	2.10E+05	0.207
4.95	6.545	2.230	2.594	0.430	2.16E+05	0.208
5.00	6.571	2.269	2.600	0.436	2.21E+05	0.209
5.05	6.598	2.293	2.606	0.440	2.25E+05	0.210
5.10	6.642	2.317	2.615	0.443	2.29E+05	0.211
5.15	6.675	2.385	2.623	0.455	2.37E+05	0.213
5.20	6.695	2.437	2.629	0.464	2.44E+05	0.214
5.25	6.736	2.471	2.637	0.468	2.49E+05	0.216
5.30	6.768	2.534	2.645	0.479	2.57E+05	0.217
5.35	6.818	2.565	2.655	0.483	2.62E+05	0.219
5.40	6.874	2.618	2.667	0.491	2.69E+05	0.221
5.45	6.912	2.700	2.677	0.504	2.79E+05	0.223
5.50	6.960	2.739	2.687	0.510	2.84E+05	0.224
5.55	7.020	2.783	2.699	0.516	2.90E+05	0.226
5.60	7.072	2.878	2.712	0.531	3.01E+05	0.228
5.65	7.133	2.960	2.725	0.543	3.11E+05	0.231
5.70	7.199	3.048	2.740	0.556	3.21E+05	0.233
5.75	7.260	3.144	2.754	0.571	3.33E+05	0.236
5.80	7.342	3.205	2.771	0.578	3.40E+05	0.238
5.85	7.413	3.336	2.788	0.598	3.55E+05	0.242
5.90	7.442	3.442	2.797	0.615	3.68E+05	0.244
5.95	7.501	3.564	2.811	0.634	3.82E+05	0.247
6.00	7.607	3.723	2.835	0.657	3.99E+05	0.251
6.05	7.675	3.890	2.853	0.682	4.18E+05	0.255
6.10	7.785	4.077	2.879	0.708	4.38E+05	0.259
6.15	7.881	4.250	2.901	0.732	4.57E+05	0.263
6.20	7.939	4.452	2.919	0.763	4.79E+05	0.268
6.25	8.035	4.619	2.941	0.785	4.98E+05	0.272

Table 10.10.1 *Continued.*

eV	ε_1	ε_2	n	k	α (cm^{-1})	R
6.30	8.117	4.826	2.963	0.814	5.20E+05	0.276
6.35	8.112	5.151	2.977	0.865	5.57E+05	0.281
6.40	8.217	5.450	3.006	0.906	5.88E+05	0.287
6.45	8.299	5.783	3.034	0.953	6.23E+05	0.294
6.50	8.256	6.186	3.047	1.015	6.69E+05	0.300
6.55	8.208	6.580	3.060	1.075	7.14E+05	0.306
6.60	8.196	6.987	3.079	1.134	7.59E+05	0.313
6.65	8.112	7.461	3.093	1.206	8.13E+05	0.320
6.70	7.889	8.038	3.094	1.299	8.82E+05	0.329
6.75	7.545	8.702	3.087	1.409	9.64E+05	0.339
6.80	7.069	9.320	3.063	1.521	1.05E+06	0.349
6.85	6.399	9.841	3.011	1.634	1.13E+06	0.358
6.90	5.505	10.21	2.924	1.746	1.22E+06	0.366
6.95	4.438	10.26	2.794	1.836	1.29E+06	0.371
7.00	3.439	10.02	2.649	1.891	1.34E+06	0.373
7.05	2.676	9.446	2.499	1.890	1.35E+06	0.368
7.10	2.192	8.704	2.363	1.842	1.33E+06	0.357
7.15	2.038	8.015	2.270	1.765	1.28E+06	0.342
7.20	2.110	7.523	2.227	1.689	1.23E+06	0.328
7.25	2.267	7.165	2.212	1.620	1.19E+06	0.316
7.30	2.370	6.871	2.195	1.565	1.16E+06	0.306
7.35	2.521	6.758	2.206	1.532	1.14E+06	0.301
7.40	2.673	6.704	2.224	1.507	1.13E+06	0.298
7.45	2.749	6.668	2.232	1.494	1.13E+06	0.296
7.50	2.878	6.635	2.248	1.476	1.12E+06	0.293
7.55	2.957	6.660	2.263	1.471	1.13E+06	0.293
7.60	2.908	6.697	2.259	1.482	1.14E+06	0.295
7.65	2.902	6.802	2.269	1.499	1.16E+06	0.298
7.70	2.901	6.988	2.288	1.527	1.19E+06	0.304
7.75	2.792	7.101	2.283	1.555	1.22E+06	0.308
7.80	2.614	7.239	2.271	1.594	1.26E+06	0.314
7.85	2.380	7.328	2.246	1.632	1.30E+06	0.319
7.90	2.099	7.361	2.208	1.667	1.33E+06	0.324
7.95	1.785	7.312	2.158	1.694	1.37E+06	0.328
8.00	1.490	7.174	2.100	1.708	1.39E+06	0.330
8.05	1.255	6.972	2.042	1.707	1.39E+06	0.329
8.10	1.092	6.748	1.991	1.695	1.39E+06	0.326
8.15	0.961	6.495	1.940	1.674	1.38E+06	0.322
8.20	0.897	6.278	1.902	1.650	1.37E+06	0.317
8.25	0.908	6.095	1.880	1.621	1.36E+06	0.311
8.30	0.929	5.910	1.859	1.590	1.34E+06	0.305
8.35	0.971	5.765	1.846	1.561	1.32E+06	0.299
8.40	1.026	5.649	1.839	1.535	1.31E+06	0.294
8.45	1.083	5.569	1.838	1.515	1.30E+06	0.290

Table 10.10.1 *Continued.*

eV	ε_1	ε_2	n	k	α (cm^{-1})	R
8.50	1.144	5.513	1.840	1.498	1.29E+06	0.286
8.55	1.198	5.467	1.843	1.483	1.29E+06	0.283
8.60	1.244	5.434	1.846	1.471	1.28E+06	0.281
8.65	1.286	5.428	1.853	1.465	1.28E+06	0.279
8.70	1.313	5.444	1.859	1.464	1.29E+06	0.279
8.75	1.325	5.475	1.865	1.468	1.30E+06	0.280
8.80	1.328	5.517	1.871	1.474	1.32E+06	0.281
8.85	1.302	5.570	1.874	1.486	1.33E+06	0.284
8.90	1.252	5.627	1.873	1.502	1.36E+06	0.287
8.95	1.177	5.675	1.867	1.520	1.38E+06	0.291
9.00	1.087	5.701	1.856	1.536	1.40E+06	0.294
9.05	0.977	5.703	1.839	1.551	1.42E+06	0.297
9.10	0.857	5.704	1.820	1.567	1.45E+06	0.301
9.15	0.754	5.697	1.803	1.580	1.47E+06	0.303
9.20	0.641	5.670	1.781	1.591	1.48E+06	0.306
9.25	0.540	5.609	1.757	1.596	1.50E+06	0.307
9.30	0.438	5.528	1.730	1.598	1.51E+06	0.308
9.35	0.323	5.429	1.697	1.599	1.52E+06	0.310
9.40	0.242	5.296	1.665	1.591	1.52E+06	0.309
9.45	0.186	5.154	1.635	1.577	1.51E+06	0.306
9.50	0.151	5.031	1.610	1.562	1.50E+06	0.304
9.55	0.163	4.924	1.595	1.543	1.49E+06	0.300
9.60	0.217	4.849	1.592	1.523	1.48E+06	0.295
9.65	0.278	4.820	1.598	1.508	1.48E+06	0.292
9.70	0.336	4.835	1.610	1.502	1.48E+06	0.290
9.75	0.364	4.854	1.617	1.501	1.48E+06	0.289
9.80	0.364	4.854	1.617	1.501	1.49E+06	0.289

*This table is an up-dated version of S. Adachi [*Optical Constants of Crystalline and Amorphous Semiconductors: Numerical Data and Graphical Information* (Kluwer Academic, Boston, 1999)] including recent data by T. Wethkamp, K. Wilmers, N. Esser, W. Richter, O. Ambacher, H. Angerer, G. Jungk, R. L. Johnson, and M. Cardona [*Thin Solid Films* **313-314**, 745 (1998)].

Table 10.10.2 *Optical constants of α-GaN for **E** // c at 300 K.**

eV	ε_1	ε_2	n	k	α (cm^{-1})	R
0.01	9.906	0.029	3.147	0.0046	4.65E+00	0.268
0.02	10.25	0.067	3.202	0.010	2.11E+01	0.275
0.03	10.96	0.130	3.311	0.020	5.97E+01	0.287
0.04	12.38	0.269	3.518	0.038	1.55E+02	0.311
0.05	15.66	0.716	3.958	0.090	4.58E+02	0.356
0.06	28.52	4.403	5.356	0.411	2.50E+03	0.472
0.062	36.76	8.649	6.104	0.708	4.45E+03	0.521
0.064	52.35	22.92	7.400	1.549	1.00E+04	0.594
0.065	62.48	44.71	8.346	2.679	1.77E+04	0.647
0.0655	63.45	64.91	8.781	3.696	2.45E+04	0.679

Table 10.10.2 *Continued.*

eV	ε_1	ε_2	n	k	α (cm^{-1})	R
0.066	52.64	91.78	8.901	5.156	3.45E+04	0.714
0.0665	20.95	113.2	8.250	6.863	4.63E+04	0.751
0.06675	-0.385	114.7	7.561	7.586	5.13E+04	0.769
0.067	-20.39	108.5	6.710	8.088	5.49E+04	0.785
0.0675	-45.28	83.03	4.965	8.362	5.72E+04	0.812
0.068	-51.23	57.74	3.603	8.013	5.52E+04	0.831
0.069	-43.30	28.39	2.059	6.895	4.82E+04	0.855
0.07	-33.40	15.89	1.339	5.933	4.21E+04	0.868
0.072	-20.79	6.766	0.733	4.618	3.37E+04	0.880
0.074	-13.97	3.674	0.487	3.770	2.83E+04	0.881
0.076	-9.841	2.292	0.363	3.158	2.43E+04	0.877
0.078	-7.097	1.561	0.291	2.680	2.12E+04	0.868
0.08	-5.150	1.130	0.247	2.283	1.85E+04	0.854
0.082	-3.701	0.854	0.221	1.936	1.61E+04	0.832
0.084	-2.583	0.668	0.206	1.620	1.38E+04	0.798
0.086	-1.695	0.536	0.203	1.318	1.15E+04	0.745
0.09	-0.376	0.366	0.273	0.671	6.12E+03	0.473
0.1	1.525	0.176	1.237	0.071	7.23E+02	0.012
0.11	2.531	0.102	1.591	0.032	3.58E+02	0.052
0.12	3.147	0.066	1.774	0.019	2.26E+02	0.078
0.13	3.559	0.046	1.886	0.012	1.60E+02	0.094
0.14	3.851	0.033	1.962	0.0085	1.20E+02	0.106
0.15	4.067	0.025	2.017	0.0062	9.45E+01	0.114
0.2	4.625	0.0086	2.151	0.0020	4.07E+01	0.133
0.3	4.961	0.0022	2.227	0.00050	1.53E+01	0.145
0.4	5.069	0.00090	2.251	0.00020	8.12E+00	0.148
0.5	5.117	0.00045	2.262	0.00010	5.06E+00	0.150
0.8	5.356		2.314			0.157
0.9	5.369		2.317			0.158
1	5.376		2.319			0.158
1.1	5.389		2.321			0.158
1.2	5.422		2.329			0.159
1.3	5.442		2.333			0.160
1.4	5.482		2.341			0.161
1.5	5.502		2.346			0.162
1.6	5.523		2.350			0.162
1.7	5.576		2.361			0.164
1.8	5.610		2.369			0.165
1.9	5.644		2.376			0.166
2	5.692		2.386			0.168
2.1	5.746		2.397			0.169
2.2	5.781		2.404			0.170
2.3	5.843		2.417			0.172
2.4	5.898		2.429			0.174

Table 10.10.2 *Continued.*

eV	ε_1	ε_2	n	k	α (cm^{-1})	R
2.5	5.989		2.447			0.176
2.6	6.066		2.463			0.178
2.7	6.179		2.486			0.182
2.8	6.264		2.503			0.184
2.9	6.394		2.529			0.188
3	6.539		2.557			0.192
3.1	6.701		2.589			0.196
3.2	6.939	0.0060	2.634	0.0011	3.57E+02	0.202
3.3	7.290	0.012	2.700	0.0023	7.69E+02	0.211
3.4	8.235	0.574	2.871	0.100	3.45E+04	0.234
3.5	7.679	1.592	2.786	0.286	1.01E+05	0.227
3.6	7.293	1.630	2.717	0.300	1.09E+05	0.218
3.7	7.147	1.676	2.691	0.311	1.17E+05	0.215
3.8	7.064	1.721	2.677	0.321	1.24E+05	0.214
3.9	6.979	1.780	2.663	0.334	1.32E+05	0.213
4	6.943	1.822	2.657	0.343	1.39E+05	0.212
4.1	6.935	1.883	2.657	0.354	1.47E+05	0.213
4.2	6.929	1.928	2.657	0.363	1.55E+05	0.213
4.3	6.922	1.974	2.657	0.371	1.62E+05	0.213
4.4	6.924	2.021	2.659	0.380	1.70E+05	0.214
4.5	6.922	2.082	2.660	0.391	1.78E+05	0.215
4.6	6.938	2.131	2.664	0.400	1.87E+05	0.216
4.7	6.986	2.178	2.674	0.407	1.94E+05	0.217
4.8	7.024	2.238	2.683	0.417	2.03E+05	0.219
4.9	7.061	2.299	2.691	0.427	2.12E+05	0.220
5	7.135	2.335	2.706	0.431	2.18E+05	0.222
5.1	7.179	2.405	2.716	0.443	2.29E+05	0.224
5.2	7.257	2.466	2.731	0.451	2.38E+05	0.227
5.3	7.343	2.529	2.749	0.460	2.47E+05	0.229
5.4	7.480	2.584	2.774	0.466	2.55E+05	0.233
5.5	7.608	2.696	2.800	0.481	2.68E+05	0.237
5.6	7.723	2.799	2.823	0.496	2.82E+05	0.240
5.7	7.891	2.887	2.854	0.506	2.92E+05	0.244
5.8	8.048	3.051	2.886	0.529	3.11E+05	0.249
5.9	8.245	3.190	2.923	0.546	3.27E+05	0.255
6	8.435	3.383	2.960	0.571	3.47E+05	0.260
6.1	8.640	3.600	3.000	0.600	3.71E+05	0.267
6.2	8.899	3.832	3.049	0.629	3.95E+05	0.274
6.3	9.118	4.098	3.091	0.663	4.23E+05	0.280
6.4	9.371	4.472	3.143	0.711	4.61E+05	0.289
6.5	9.667	4.846	3.200	0.757	4.99E+05	0.297

*This table is an up-dated version of S. Adachi [*Optical Constants of Crystalline and Amorphous Semiconductors: Numerical Data and Graphical Information* (Kluwer Academic, Boston, 1999)] including recent data by C. H. Yan, H. W. Yao, J. M. Van Hove, A. M. Wowchak, P. P. Chow, J. Han, and J. M. Zavada [*Mat. Res. Soc. Symp. Proc.* **591**, 313 (2000)].

10.10.2 The Reststrahlen Region

• Static and high-frequency dielectric constants

Table 10.10.3 *Static and high-frequency dielectric constants ε_s and ε_∞ for α-GaN.*

$E \perp c$		$E \parallel c$		Comment
ε_s	ε_∞	ε_s	ε_∞	
12±2	5.8	12±2	5.8	Bulk crystal, T=300 K [10.1]
	5.2±0.2			Bulk crystal, T=300 K [10.2]
9.5	5.35	10.4	5.35	Epilayer on Al_2O_3, T=300 K [10.3]
	5.76			Bulk crystal, T=300 K [10.4]
8.9±0.3	5.2±0.1	9.8±0.3	5.2±0.1	Epilayer on Al_2O_3, T=300 K [10.5]
9.38	5.35	10.2	5.35	Epilayer on Al_2O_3, T=300 K [10.6]
8.94	5.15			Epilayer on Al_2O_3, T=300 K [10.7]
9.04	5.14			Epilayer on Al_2O_3, T=300 K [10.8]
	5.20		5.18	Epilayer on Al_2O_3, T=300 K [10.9]
9.6	5.4	10.6	5.4	Mean value

[10.1] D. D. Manchon, Jr., A. S. Barker, Jr., P. J. Dean, and R. B. Zetterstrom, *Solid State Commun.* **8**, 1227 (1970).
[10.2] E. Ejder, *Phys. Status Solidi A* **6**, 445 (1971).
[10.3] A. S. Barker and M. Ilegems, *Phys. Rev. B* **7**, 743 (1973).
[10.4] P. Perlin, I. Gorczyca, N. E. Christensen, I. Grzegory, H. Teisseyre, and T. Suski, *Phy.s. Rev. B* **45**, 13307 (1992).
[10.5] H. Sobotta, H. Neumann, R. Franzheld, and W. Seifert, *Phys. Status Solidi B* **174**, K57 (1992).
[10.6] T. Azuhata, T. Sota, K. Suzuki, and S. Nakamura, *J. Phys.: Condens. Matter* **7**, L129 (1995).
[10.7] G. Yu, H. Ishikawa, M Umeno, T. Egawa, J. Watanabe, T. Soga, and T. Jimbo, *J. Appl. Phys.* **73**, 1472 (1998).
[10.8] T. Deguchi, D. Ichiryu, K. Toshikawa, K. Sekiguchi, T. Sota, R. Matsuo, T. Azuhata, M. Yamaguchi, T. Yagi, S. Chichibu, and S. Nakamura, *J. Appl. Phys.* **86**, 1860 (1999).
[10.9] A. Kasic, M. Schubert, S. Einfeldt, D. Hommel, and T. E. Tiwald, *Phys. Rev. B* **62**, 7365 (2000).

The pressure dependence of the high-frequency dielectric constant ε_∞ for α-GaN has also been investigated theoretically by J.-M. Wagner and F. Bechstedt [*Phys. Rev. B* **62**, 4526 (2000)].

• Reststrahlen parameter

Table 10.10.4 *A set of the reststrahlen parameters for α-GaN at 300 K.*

$$\varepsilon(\omega) = \varepsilon_\infty \left(1 + \frac{\omega_{LO}^2 - \omega_{TO}^2}{\omega_{TO}^2 - \omega^2 - i\omega\gamma} \right)$$

$E \perp c$				$E \parallel c$				Comment
ε_∞	ω_{LO} (cm^{-1})	ω_{TO} (cm^{-1})	γ (cm^{-1})	ε_∞	ω_{LO} (cm^{-1})	ω_{TO} (cm^{-1})	γ (cm^{-1})	
5.8	770	540		5.8	800	560		Bulk crystal [10.10]
5.35	746	560	17	5.35	744	533	17	α-GaN/Al_2O_3 [10.11]
5.2	741	565	10.2	5.2	738	538	9.7	α-GaN/Al_2O_3 [10.12]
5.35	744	560	10	5.35	740	530	11	α-GaN/GaAs(001) [10.13]

Table 10.10.4 *Continued.*

$E \perp c$				$E \parallel c$				Comment
ε_∞	ω_{LO} (cm^{-1})	ω_{TO} (cm^{-1})	γ (cm^{-1})		ω_{LO} (cm^{-1})	ω_{TO} (cm^{-1})	γ (cm^{-1})	
5.35	744	560	6	5.35	740	530	7	α-GaN/GaAs(111) [10.13]
5.35	744	560	38	5.35	739	529	65	α-GaN/GaP(001) [10.13]
5.15	737.6	559.7	4.9					α-GaN/Al_2O_3 [10.14]
5.14	740	558	3.5					α-GaN/Al_2O_3 [10.15]
5.2	735	560	5	5.2	742	533	5	α-GaN/Si(001) [10.16]

[10.10] D. D. Manchon, Jr., A. S. Barker, Jr., P. J. Dean, and R. B. Zetterstrom, *Solid State Commun.* **8**, 1227 (1970).
[10.11] A. S. Barker and M. Ilegems, *Phys. Rev. B* **7**, 743 (1973).
[10.12] H. Sobotta, H. Neumann, R. Franzheld, and W. Seifert, *Phys. Status Solidi B* **174**, K57 (1992).
[10.13] G. Mirjalili, T. J. Parker, S. F. Shayesteh, M. M. Bülbül, S. R. P. Smith, T. S. Cheng, and C. T. Foxon, *Phys. Rev. B* **57**, 4656 (1998).
[10.14] G. Yu, H. Ishikawa, M Umeno, T. Egawa, J. Watanabe, T. Soga, and T. Jimbo, *J. Appl. Phys.* **73**, 1472 (1998).
[10.15] T. Deguchi, D. Ichiryu, K. Toshikawa, K. Sekiguchi, T. Sota, R. Matsuo, T. Azuhata, M. Yamaguchi, T. Yagi, S. Chichibu, and S. Nakamura, *J. Appl. Phys.* **86**, 1860 (1999).
[10.16] Y. T. Hou, Z. C. Feng, J. Chen, X. Zhang, S. J. Chua, and J. Y. Lin, *Solid State Commun.* **115**, 45 (2000).

• Multiphonon optical absorption spectra

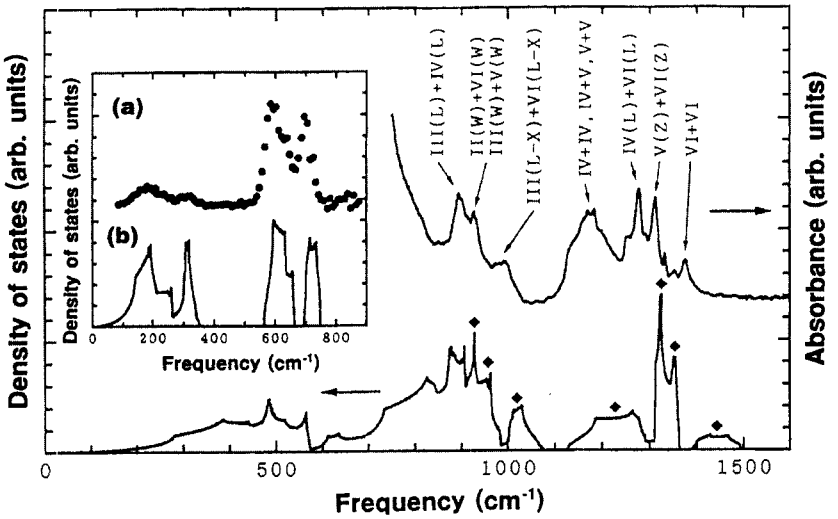

Fig. 10.10.4 Two-phonon absorption spectrum of α-GaN at 300 K (upper curve) and calculated two-phonon density of states of β-GaN for sum combinations including overtones (lower curve). The strong absorption below 800 cm^{-1} is due to the reststrahlen band. The solid diamonds represent seven structures corresponding to those indicated by arrows in the two-phonon absorption spectrum. The inset shows (a) neutron-weighted phonon density of states of α-GaN and (b) phonon density of states calculated for β-GaN with an adiabatic bond-charge model. [From T. Azuhata, K. Shimada, T. Deguchi, T. Sota, K. Suzuki, S. Chichibu, and S. Nakamura, *Jpn. J. Appl. Phys.* **38**, L151 (1999).]

10.10.3 At or Near the Fundamental Absorption Edge

• Free-exciton binding energy and related parameters

Table 10.10.5 *Free-exciton binding (Rydberg) energy G for α-GaN. PLE=photoluminescence excitation spectroscopy; PL=photoluminescence; R=reflectivity; PR=photoreflectance; TPS=two-photon spectroscopy; OA=optical absorption.*

G (meV)			Comment
A	*B*	*C*	
28^{+6}_{-3}			PLE, T=1.6 K [10.17]
27			PLE, T=4.2 K [10.18]
20			PL, T=10 K [10.19]
18.3			PL, T=10 K [10.20]
20	22		PL, T=2 K [10.21]
26.7±0.5			PL, T=1.5 K [10.22]
25.3			PR, T=10 K [10.23]
21±1	21±1	23±1	R, PR, T=10 K [10.24]
22.7			PL, T=6, 25 K [10.25]
20	18.5		PL, R, PR, T=2 K [10.26]
26.1±0.7			PL, T=1.8 K [10.27]
26			PR, T=10 K [10.28]
27.1±0.6	27.6±0.7	29.1±1.3	TPS, T=7 K [10.29]
20.4±0.5	20.4±0.5	23.5±0.5	OA, T=77 K [10.30]
26.4			PL, T=1.7 K [10.31]
25±2			PL, R, T=9 K [10.32]
24.7	24.0	22.4	PL, R, T=1.7 K [10.33]
25±1	25±1		R, PR, T=2 K [10.34]
25.5			PL, R, T=10 K [10.35]
23.44	23.6		R, T=10 K [10.36]
26			PL, T=12 K [10.37]
24.0	22.8	24.5	Mean value

[10.17] B. Monemar, *Phys. Rev. B* **10**, 676 (1974).
[10.18] T. Ogino and M. Aoki, *Jpn. J. Appl. Phys.* **19**, 2395 (1980).
[10.19] .M. Smith, G. D. Chen, J. Z. Li, J. Y. Lin, H. X. Jiang, A. Salvador, W. K. Kim, O. Aktas, A. Botchkarev, and H. Morkoç, *Appl. Phys. Lett.* **67**, 3387 (1995).
[10.20] M. Smith, G. D. Chen, J. Y. Lin, H. X. Jiang, M. Asif Khan, C. J. Sun, Q. Chen, and J. W. Yang, *J. Appl. Phys.* **79**, 7001 (1996).
[10.21] D. C. Reynolds, D. C. Look, W. Kim, Ö. Aktas, A. Botchkarev, A. Salvador, H. Morkoç, and D. N. Talwar, *J. Appl. Phys.* **80**, 594 (1996).
[10.22] D. Volm, K. Oettinger, T. Streibl, D. Kovalev, M. Ben-Chorin, J. Diener, B. K. Meyer, J. Majewski, L.Eckey, A. Hoffmann, H. Amano, I. Akasaki, K. Hiramatsu, and T. Detchprohm, *Phys. Rev. B* **53**, 16543 (1996)
[10.23] S. Chichibu, A. Shikanai, T. Azuhata, T. Sota, A. Kuramata, K. Horino, and S. Nakamura, *Appl. Phys. Lett.* **68**, 3766 (1996).
[10.24] W. Shan, B. D. Little, A. J. Fischer, J. J. Song, and B. Goldenberg, *Phys. Rev. B* **54**, 16369 (1996).
[10.25] J. A. Freitas, Jr., K. Doverspike, and A. E. Wickenden, *Mat. Res. Soc. Symp. Proc.* **395**, 485 (1996).
[10.26] M. Tchounkeu, O. Briot, B. Gil, J. P. Alexis, and R.-L. Aulombard, *J. Appl. Phys.* **80**, 5352 (1996).

[10.27] C. Merz, M. Kunzer, U. Kaufmann, I. Akasaki, and H. Amano, *Semicond. Sci. Technol.* **11**, 712 (1996).
[10.28] A. Shikanai, T. Azuhata, T. Sota, S. Chichibu, A. Kuramata, K. Horino, and S. Nakamura, *J. Appl. Phys.* **81**, 417 (1997).
[10.29] M. Steube, K. Reimann, D. Fröhlich, and S. J. Clarke, *Appl. Phys. Lett.* **71**, 948 (1997).
[10.30] J. F. Muth, J. H. Lee, I. K. Shmagin, R. M. Kolbas, H. C. Casey, Jr., B. P. Keller, U. K. Mishra, and S. P. DenBaars, *Appl. Phys. Lett.* **71**, 2572 (1997).
[10.31] B. J. Skromme, H. Zhao, B. Goldenberg, H. S. Kong, M. T. Leonard, G. E .Bulman, C. R. Abernathy, and S. J. Pearton, *Mat. Res. Soc. Symp. Proc.* **449**, 713 (1997).
[10.32] M. Leroux, B. Beaumont, N. Grandjean, C. Golivet, P. Gibart, J. Massies, J. Leymarie, A. Vasson, and A. M. Vasson, *Mater. Sci. Eng. B* **43**, 237 (1997).
[10.33] B. J. Skromme, *Mater. Sci. Eng. B* **50**, 117 (1997).
[10.34] A. Alemu, B. Gil, M. Julier, and S. Nakamura, *Phys. Rev. B* **57**, 3761 (1998).
[10.35] Z. X. Liu, S. Pau, K. Syassen, J. Kuhl, W. Kim, H. Morkoç, M. A. Khan, and C. J. Sun, *Phys. Rev. B* **58**, 6696 (1998).
[10.36] K. Torii, T. Deguchi, T. Sota, K. Suzuki, S. Chichibu, and S. Nakamura, *Phys. Rev. B* **60**, 4723 (1999).
[10.37] A. K. Viswanath, J. I. Lee, S. Yu, D. Kim, Y. Choi, and C. Hong, *J. Appl. Phys.* **84**, 3848 (1998).

Table 10.10.6 *Free-exciton parameters (G=binding energy; a_B=1st-orbital Bohr radius; μ=reduced mass) at the fundamental absorption edge of α-GaN.*

Exciton	G (meV)	a_B (Å)*	μ (m_0)*
A	24.0	31	0.164
B	22.8	33	0.156
C	24.5	31	0.168

*Calculated.

The free-exciton binding energy G as a function of hydrostatic pressure p for α-GaN measured by Z. X. Liu, S. Pau, K. Syassen, J. Kuhl, W. Kim, H. Morkoç, M. A. Khan, and C. J. Sun [*Phys. Rev. B* **58**, 6696 (1998)] provides the linear pressure coefficient of dG/dp=0.6 meV/GPa.

Table 10.10.7 *Spin-exchange interaction constant j for α-GaN.*

j (meV)	Ref.
0.6±0.1	[10.38]
0.58±0.05	[10.39]

[10.38] M. Julier, J. Campo, B. Gil, J. P. Lascaray, and S. Nakamura, *Phys. Rev. B* **57**, R6791 (1998).
[10.39] P. P. Paskov, T. Paskova, P. O. Holtz, and B. Monemar, *Phys. Rev. B* **64**, 115201 (2001).

- **Refractive index**

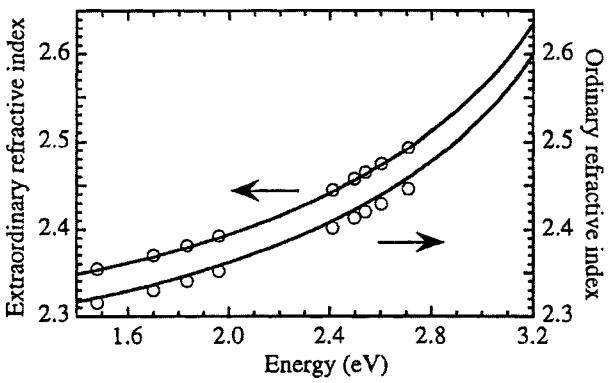

Fig. 10.10.5 Ordinary- ($E \perp c$) and extraordinary-ray ($E \| c$) refractive indices for α-GaN grown on (0001) sapphire (open circles) and 6H-SIC(0001) substrates (solid lines). The open circles were measured by M. J. Bergmann, Ü. Özgür, H. C. Casey, Jr., H. O. Everitt, and J. F. Muth [*Appl. Phys. Lett.* **75**, 67 (1999)]. [From R. Goldhahn, S. Shokhovets, J. Scheiner, G. Gobsch, T. S. Cheng, C. T. Foxon, U. Kaiser, G. D. Kipshidze, and W. Richter, *Phys. Status Solidi A* **177**, 107 (2000).]

• **Refractive index: Temperature dependence**

Table 10.10.8 *Temperature coefficient of the refractive index, $n^{-1}(dn/dT)$, in the long- wavelength limit for α-GaN ($\mathbf{E}\perp c$) [10.40].*

$\frac{1}{n}\frac{dn}{dT}$ (10^{-5} K^{-1})
2.6

[10.40] See, S. Adachi, *Optical Properties of Crystalline and Amorphous Semiconductors: Materials and Fundamental Properties* (Kluwer Academic, Boston, 1999).

The refractive-index dispersion as a function of temperature for α-GaN has also been measured by L. Siozade, S. Colard, M. Mihailovic, J. Leymarie, A. Vasson, N. Grandjean, M. Leroux, and J. Massies [*Jpn. J. Appl. Phys.* **39**, 20 (2000)].

• **Refractive index: Pressure dependence**

Table 10.10.9 *Pressure coefficient of the refractive index $n^{-1}(dn/dp)$ in the long-wavelength limit for α-GaN ($\mathbf{E}\perp c$) at 300 K [10.41].*

$\frac{1}{n}\frac{dn}{dp}$ (10^{-2} GPa^{-1})
−0.30±0.04

[10.41] P. Perlin, I. Gorczyca, N. E. Christensen, I. Grzegory, H. Teisseyre, and T. Suski, *Phys. Rev. B* **45**, 13307 (1992).

• **Fundamental absorption edge**

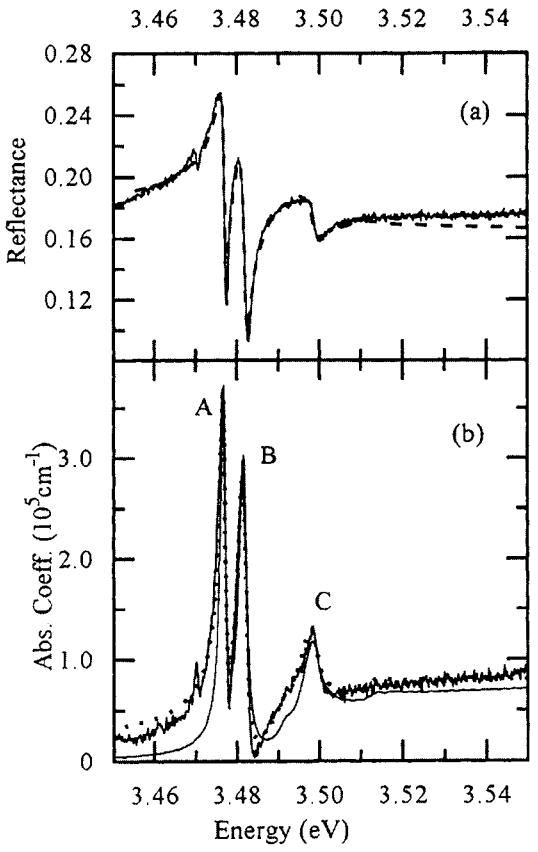

Fig. 10.10.6 (a) Experimental reflectance spectrum of an α-GaN/GaN epilayer at T=1.8 K, solid line, and the best-fit theoretical curve, dashed line. (b) Optical absorption spectrum of α-GaN obtained from Kramers–Kronig analysis of reflectance spectrum in (a), solid line, obtained from the exciton–polariton model, dotted line, and expected "bulk" absorption, thin solid line. [From R. Stępniewski, K. P. Korona, A. Wysmołek, J. M. Baranowski, K. Pakuła, M. Potemski, G. Martinez, I. Grzegory, and S. Porowski, *Phys. Rev. B* **56**, 15151 (1997).]

• **Fundamental absorption edge: Temperature dependence**

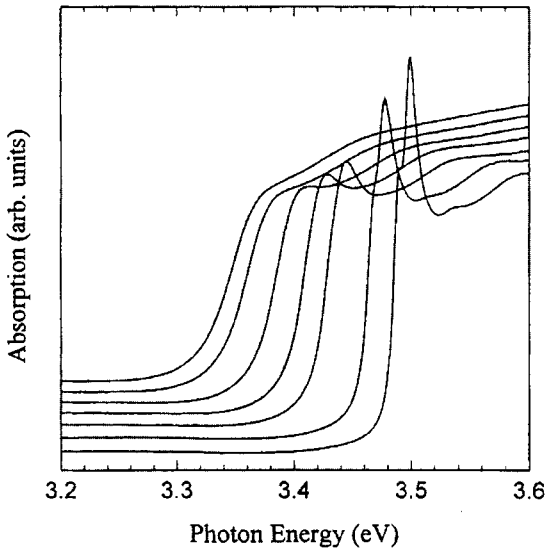

Fig. 10.10.7 Optical absorption spectra for 0.38-μm-thick α-GaN epilayer grown on (0001) sapphire substrate measured at selected temperatures (from right to left, 100, 200, 300, 350, 400, 450, and 475 K). These data clearly show that the exciton peak is observed well above room temperature. [From A. J. Fischer, W. Shan, J. J. Song, Y. C. Chang, R. Horning, and B. Goldenberg, *Appl. Phys. Lett.* **71**, 1981 (1997).]

• **Fundamental absorption edge: Urbach tail**

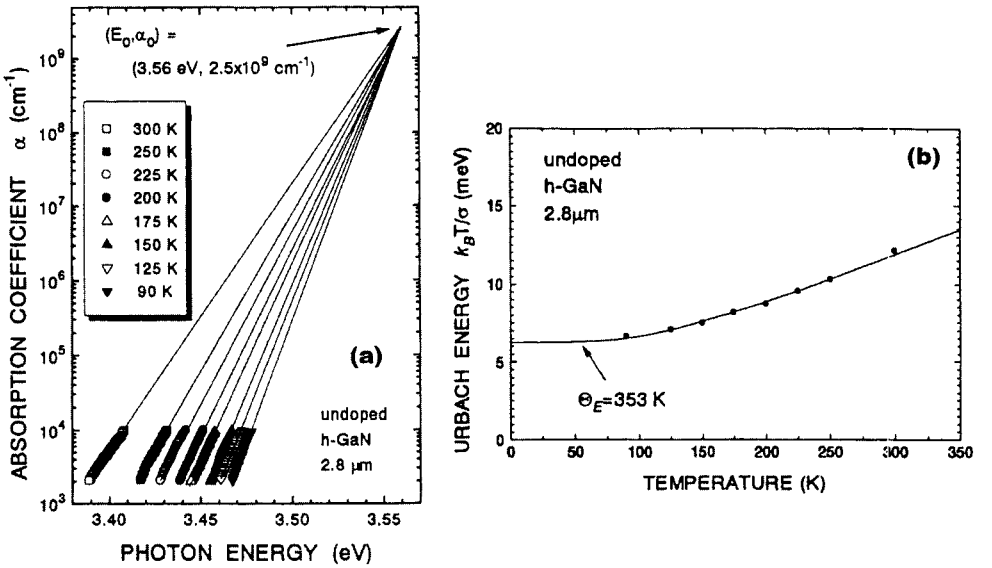

Fig. 10.10.8 (a) Optical absorption spectra for α-GaN (h-GaN) at different temperatures. The point (E_0, α_0) represents a converging point. (b) Urbach energy (parameter) as a function of temperature. [From S. Chichibu, T. Mizutani, T. Shioda, H. Nakanishi, T. Deguchi, T. Azuhata, T. Sota, and S. Nakamura, *Appl. Phys. Lett.* **70**, 3440 (1997).]

• **Fundamental absorption edge: Pressure dependence**

The transmission spectra ($\boldsymbol{E}\perp c$) near the fundamental absorption edge of α-GaN under hydrostatic pressure has been measured by P. Perlin, I. Gorczyca, N. E. Christensen, I. Grzegory, H. Teisseyre, and T. Suski [*Phy.s. Rev. B* **45**, 13307 (1992)].

10.10.4 The Interband Transition Region

• Fundamental optical spectra

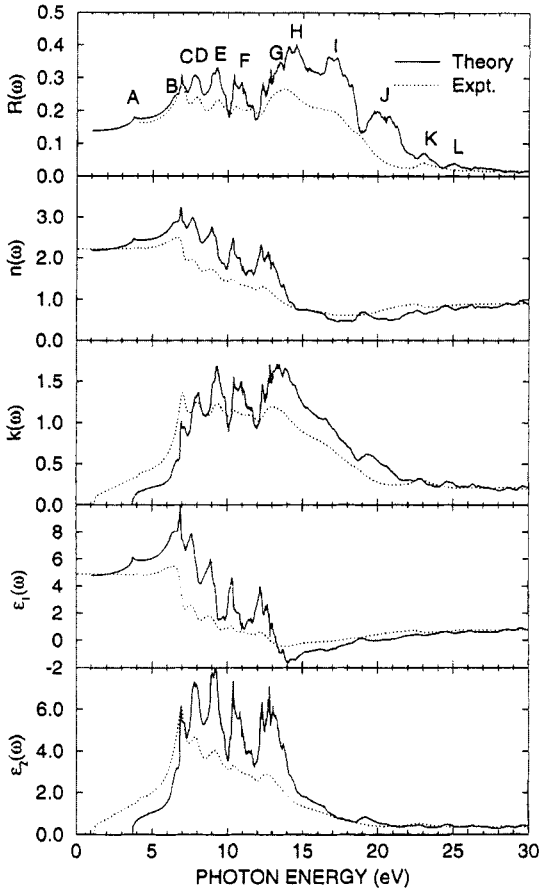

Fig. 10.10.9 Complex dielectric function, $\varepsilon(E)=\varepsilon_2(E)+i\varepsilon_2(E)$, complex refractive index, $n^*(E)=n(E)+ik(E)$, and reflectivity, $R(E)$, for α-GaN, solid lines (theory), dotted line (experiment). All theoretical curves are shifted upwards by 0.98 eV. All curves correspond to $\boldsymbol{E}\perp c$. [From W. R. L. Lambrecht, B. Segall, J. Rife, W. R. Hunter, and D. K. Wickenden, *Phys. Rev. B* **51**, 13516 (1995).]

• $\varepsilon(E)$ spectrum: External perturbation and/or doping effects

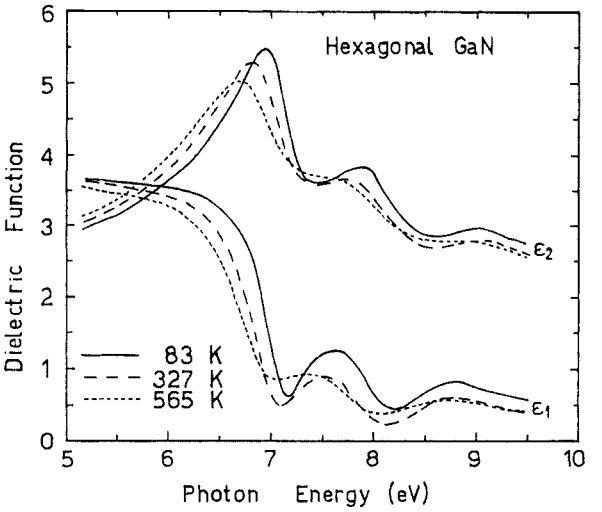

Fig. 10.10.10 Dielectric-function spectra for α-GaN measured at three different temperatures, T=83, 327, and 565 K. [From S. Logothetidis, J. Petalas, M. Cardona, and T. D. Moustakas, *Phys. Rev. B* **50**, 18017 (1994).]

10.10.5 Free-Carrier Absorption and Related Phenomena

No detailed data are available for α-GaN.

10.11 ELASTOOPTIC, ELECTROOPTIC, AND NONLINEAR OPTICAL PROPERTIES

10.11.1 Elastooptic Effect

• Photoelastic constant

Table 10.11.1 *Photoelastic constant p_{ij} in the static limit ($E \to 0$ eV) for α-GaN [11.1].*

p_{11}	p_{12}	p_{13}	p_{33}	p_{44}	p_{66}
0.031	0.008	0.006	0.033	0.010	0.012

[11.1] Estimated [S. Yu. Davydov and S. K. Tikhonov, *Semicond.* **31**, 698 (1997)].

10.11.2 Linear Electrooptic Constant

Table 10.11.2 *Linear electrooptic constant r_{ij} for α-GaN [11.2].*

Energy (eV)	Wavelength (μm)	r_{ij} (pm/V)		
		r_{13}	r_{33}	r_{42}
1.958	0.633	0.57±0.11	1.91±0.35	

[11.2] X.-C. Long, R. A. Myers, S. R. J. Brueck, R. Ramer, K. Zheng, and S. D. Hersee, *Appl. Phys. Lett.* **67**, 1349 (1995).

10.11.3 Quadratic Electrooptic Constant

No detailed data are available for α-GaN.

10.11.4 Franz–Keldysh Effect

No detailed data are available for α-GaN.

10.11.5 Nonlinear Optical Constant

• Second-order nonlinear optical susceptibility

Table 10.11.3 *Theoretical second-order nonlinear optical susceptibility d_{ij} in the static limit ($\hbar\omega \to 0$ eV) for α-GaN.*

d_{ij} (pm/V)			Ref.
d_{15}	d_{31}	d_{33}	
−2.14		3.02	[11.3]
−2.1		3.5	[11.4]
−2.2		2.8	[11.5]
−2.9		5.2	[11.6]

[11.3] Local-density approximation plus scissors [J. L.P. Hughes, Y. Wang, and J. E. Sipe, *Phys. Rev. B* **55**, 13630 (1997)].

[11.4] Local-density approximation plus scissors [J. Chen, L. Jönsson, J. W. Wilkins, and Z. H. Levine, *Phys. Rev. B* **56**, 1787 (1997)].
[11.5] Local-density approximation plus scissors [S. N. Rashkeev, W. R. L. Lambrecht, and B.Segall, *Phys. Rev. B* **57**, 3905 (1998)].
[11.6] First-principle full-potential linearized augmented plane-wave method [V. I. Gavrilenko and R. Q. Wu, *Phys. Rev. B* **61**, 2632 (2000)].

Table 10.11.4 *Experimental second-order nonlinear optical susceptibility d_{ij} for α-GaN.*

d_{ij} (pm/V)			Comment
d_{15}	d_{31}	d_{33}	
2.7	2.7	−5.4	λ=532 nm [11.7]
	5±2	−10±3	λ=633 nm [11.8]
8.0±0.7	8.2±0.7	−16.5±1.3	λ=1064 nm [11.9]
|7.2±0.1|	|7.4±0.1|	|14.9±0.4|	λ=1064 nm [11.10]

[11.7] I. Miragliotta, D. K. Wickenden, T. J. Kistenmacher, and W. A. Bryden, *J. Opt. Soc. Am. B* **10**, 1447 (1993).
[11.8] X.-C. Long, R. A. Myers, S. R. J. Brueck, R. Ramer, K. Zheng, and S. D. Hersee, *Appl. Phys. Lett.* **67**, 1349 (1995)].
[11.9] H. Y. Zhang, X. H. He, Y. H. Shih, M. Schurman, Z. C. Feng, and R. A. Stall, *Appl. Phys. Lett.* **69**, 2953 (1996).
[11.10] T. Fujita, T. Hasegawa, M. Haraguchi, T. Okamoto, M. Fukui, and S. Nakamura, *Jpn. J. Appl. Phys.* **39**, 2610 (2000).

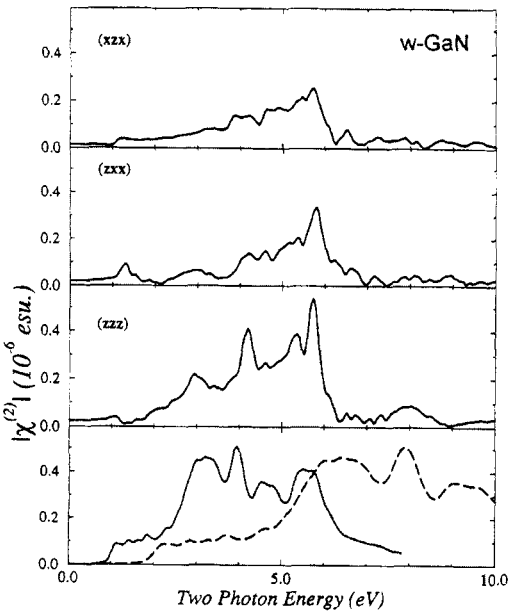

Fig. 10.11.1 Calculated absolute second-order nonlinear optical susceptibility, $|\chi^{(2)}(-2\omega,\omega,\omega)|$, for α-GaN (*w*-GaN). The calculated $\varepsilon_2(\omega)$ (solid line) and $\varepsilon_2(\omega/2)$ spectra (dashed line) are also shown in the bottom panel. [From V. I. Gavrilenko and R. Q. Wu, *Phys. Rev. B* **61**, 2632 (2000).]

• Third-order nonlinear optical susceptibility

Table 10.11.5 *Third-order nonlinear optical susceptibility $\chi^{(3)}_{3223}(-2\omega;\omega,\omega,0)$ for α-GaN.*

$\chi^{(3)}_{3223}$ (10^{-19} m^2/V^2)	Comment
5.3	Exper. [11.11]

[11.11] At the 3.43-eV resonance [J. Miragliotta and D. K. Wickenden, *Phys. Rev. B* **53**, 1388 (1996)].

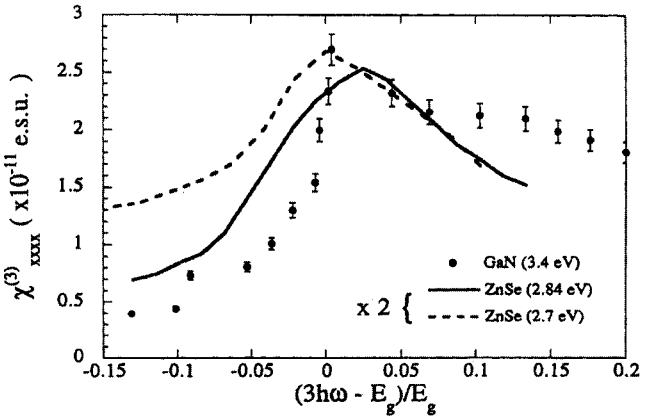

Fig. 10.11.2 Experimental third-order optical susceptibility, $|\chi^{(3)}_{xxxx}(-3\omega;\omega,\omega,\omega)|$ ($|\chi^{(3)}_{1111}(-3\omega;\omega,\omega,\omega)|$), for α-GaN (solid circles), together with the theoretical predictions of this susceptibility in ZnSe (solid and dashed lines). The solid and dashed lines are scaled by a factor of 2 with respect to the GaN data. [From J. Miragliotta and D. K. Wickenden, *Phys. Rev. B* **50**, 14960 (1994).]

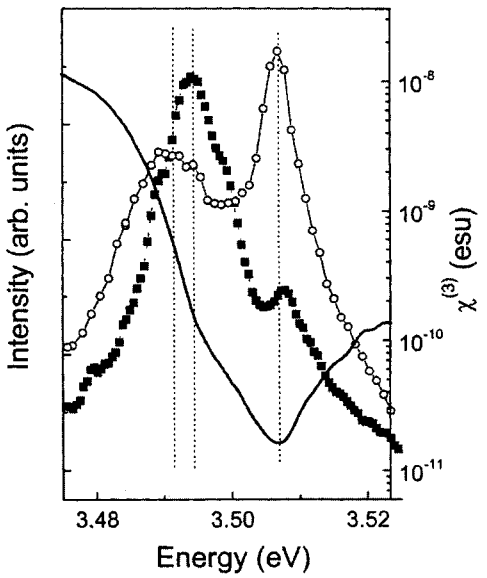

Fig. 10.11.3 (○): $\chi^{(3)}$ values determined from degenerate four-wave mixing measurements in a two-wave configuration. The data are corrected for the absorption of the sample. Solid line: transmission spectrum. (■): luminescence spectrum. All results are obtained for an intensity of excitation of 4 kV/cm^2 at low temperature (2 K). The maximum optical absorption is $\alpha \sim 10^6$ cm^{-1} at $\hbar\omega$=3.507 eV, The dotted lines show the spectral positions of the D_0, A, and B excitons. [From H. Haag, P. Gilliot, R. Lévy, B. Hönerlage, O. Briot, S. Ruffenach-Clur, and R. L. Aulombard, *Appl. Phys. Lett.* **74**, 1436 (1999).]

• Two-photon optical absorption

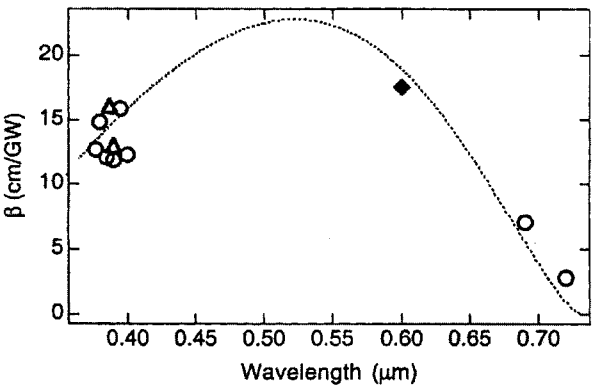

Fig. 10.11.4 Two-photon absorption coefficient β as a function of wavelength in α-GaN. The symbols show the experimental data and the solid line represents the theoretical dispersion. [From C.-K. Sun, J.-C. Liang, J.-C. Wang, F.-J. Kao, S. Keller, M. P. Mack, U. Mishra, and S. P. DenBaars, *Appl. Phys. Lett.* **76**, 439 (2000).]

10.12 CARRIER TRANSPORT PROPERTIES

10.12.1 Low-Field Mobility: Electrons

Table 10.12.1 *300-K (μ_{300K}) and peak Hall mobilities (μ_{peak}) for electrons in α-GaN.*

Mobility	Value ($cm^2/V\,s$)	Comment
μ_{300K}	1245	[12.1]
μ_{peak}	~7400	T~60 K [12.1]
	~8000	T~40 K [12.2]

[12.1] D. C. Look and J. R. Sizelove, *Appl. Phys. Lett.* **79**, 1133 (2001).
[12.2] Obtained from an analysis of magnetic-field-dependent Hall-effect data by assuming a two-layer model [A. Saxler, D. C. Look, S. Elhamri, J. Sizelove, W. C. Mitchel, C. M. Sung, S. S. Park, and K. Y. Lee, *Appl. Phys. Lett.* **78**, 1873 (2001)].

- **Temperature dependence**

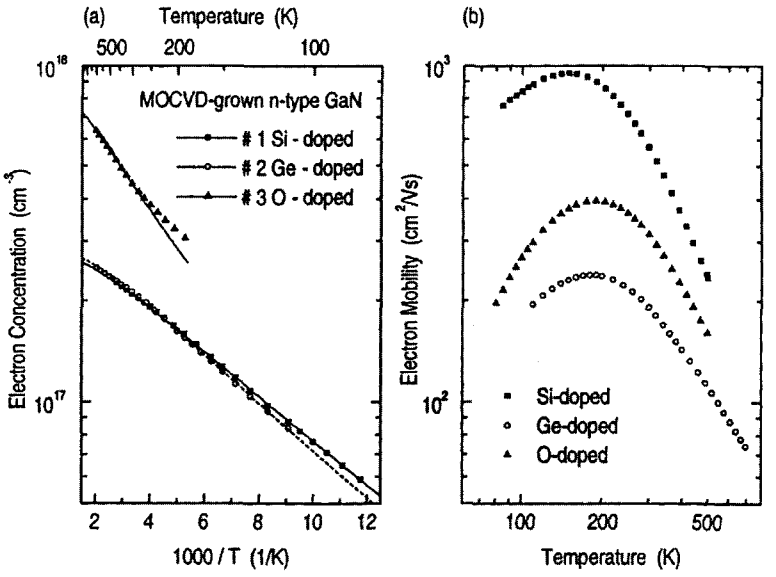

Fig. 10.12.1 Temperature variation of (a) electron concentration and (b) electron mobility for Si-, Ge-, and O-doped, *n*-type α-GaN samples grown by MOCVD. [From W. Götz, R. S. Kern, C. H. Chen, H. Liu, D. A. Steigerwald, and R. M. Fletcher, *Mater. Sci. Eng. B* **59**, 211 (1999).]

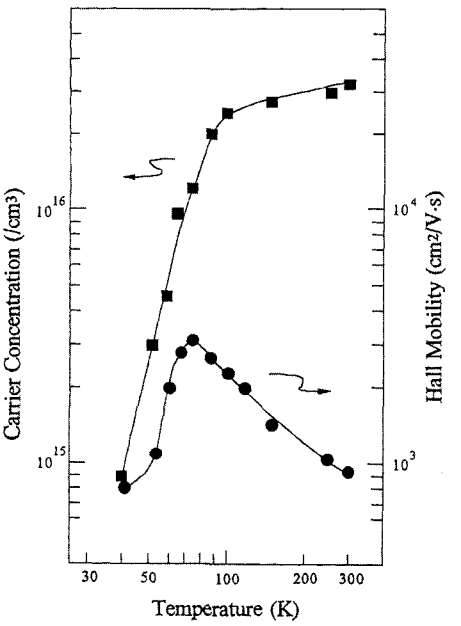

Fig. 10.12.2 Temperature variation of carrier concentration and Hall mobility for undoped, *n*-type α-GaN sample grown on a GaN-buffer/Al_2O_3 substrate by MOCVD. [From S. Nakamura, T. Mukai, and M. Senoh, *J. Appl. Phys.* **71**, 5543 (1992).]

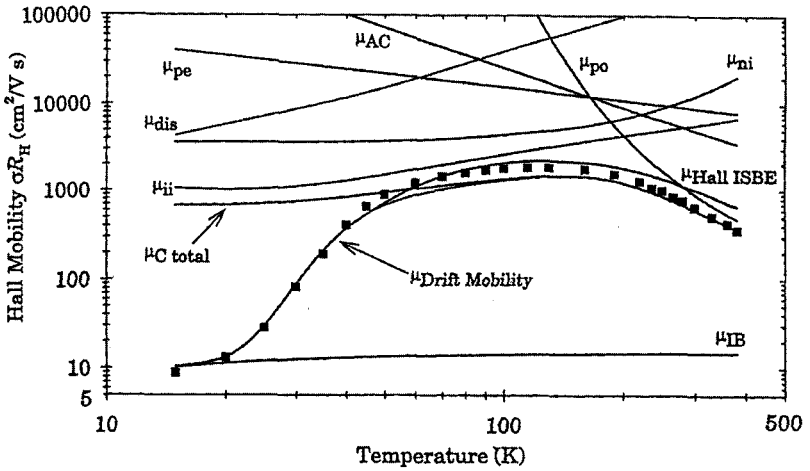

Fig. 10.12.3 Hall mobility versus temperature for α-GaN. The solid squares show the experimental data obtained from a nominally undoped sample grown on an SiC-buffer/Al_2O_3 substrate. The solid lines represent the drift mobilities for scattering by optical phonons (μ_{op}), neutral impurities (μ_{ni}), acoustic phonons (μ_{AC}), dislocations (μ_{dis}), ionized impurities (μ_{ii}), and piezoelectric scattering (μ_{pe}). μ_{IB} represents the mobility of electrons in an impurity band. μ_{Ctot} represents the drift mobility in the conduction band calculated in the relaxation approximation, where $\mu_{HallISBE}$ is the Hall mobility calculated by iterative solution of the Boltzmann equation. [From H. Eshghi, D. Lacefield, B. Beaumont, and P. Gibart, *Phys. Status Solidi* **216**, 733 (1999).]

- **Donor concentration (free-carrier) dependence**

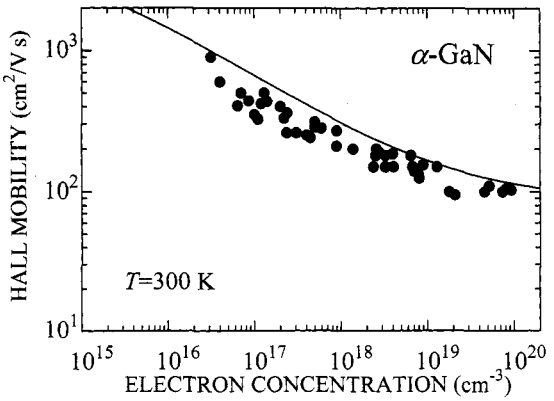

Fig. 10.12.4 Electron Hall mobility μ versus electron concentration n for n-type α-GaN at 300 K. The experimental data are taken from S. N. Mohammad, A. A. Salvador, and H. Morkoç [*Proc. IEEE* **83**, 1306 (1995)]. The solid line represents the calculated result with $\mu = 85 + 5215/[1 + (n/10^{15})^{0.45}]$, where n is in cm^{-3} and μ is in cm^2/V s.

- **Hall factor**

The Hall factor for α-GaN has been obtained theoretically by D. L. Rode [*Phys. Status Solidi B* **55**, 687 (1973)], and its value is reported to be $\gamma \sim 1.15$ at T=300 K.

10.12.2 Low-Field Mobility: Holes

Table 10.12.2 *300-K (μ_{300K}) and peak Hall mobilities (μ_{peak}) for holes in α-GaN.*

Mobility	Value (cm^2/V s)	Comment
μ_{300K}	370	[12.3]
μ_{peak}	500	$p \sim 5\times10^{11}$ cm^{-3}, $T \sim 250$ K [12.3]

[12.3] See, J. W. Orton and C. T. Foxon, *Rep. Prog. Phys.* **61**, 1 (1998).

• **Temperature dependence**

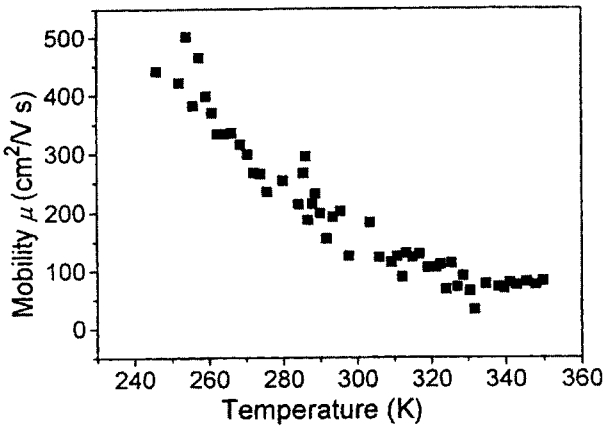

Fig. 10.12.5 Hall mobility versus temperature for undoped, p-type α-GaN grown on Al_2O_3 by MBE. [From M. Rubin, N. Newman, J. S. Chan, T. C. Fu, and J. T. Ross, *Appl. Phys. Lett.* **64**, 64 (1994).]

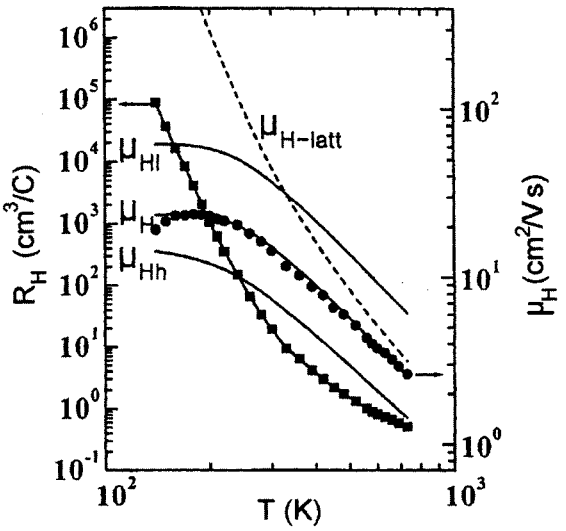

Fig. 10.12.6 Experimental Hall-effect data and theoretical curves as a function of temperature T for α-GaN. The Mg-doped, p-type α-GaN sample was grown on an Al_2O_3 substrate. μ_{Hl} and μ_{Hh} represent the Hall mobilities of light and heavy holes, respectively, and $\mu_{H\text{-latt}}$ represents the combined Hall mobility taking into account lattice scattering only. [From K. S. Kim, M. G. Cheong, C.-H. Hong, G. M. Yang, K. Y. Lim, E.-K. Suh, and H. J. Lee, *Appl. Phys. Lett.* **76**, 1149 (2000).]

• **Acceptor concentration (free-carrier) dependence**

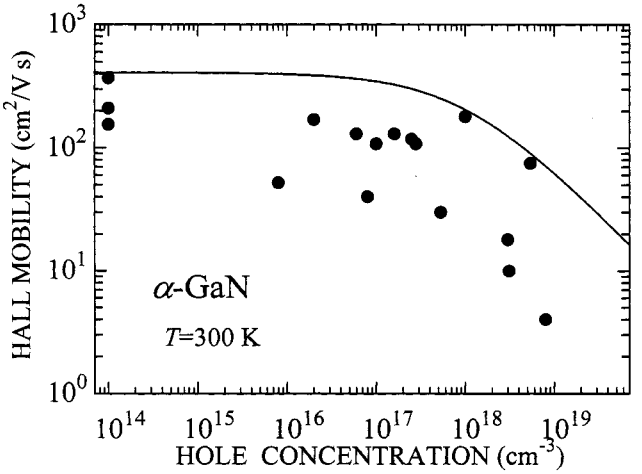

Fig. 10.12.7 Hole Hall mobility μ versus hole concentration p in p-type α-GaN at 300 K. The experimental data are taken from various sources. The solid line represents the calculated result with $\mu = 410/[1+(p/10^{18})^{0.75}]$, where p is in cm^{-3} and μ is in cm^2/V s.

• **Hall factor**

The Hall factor as a function of temperature for α-GaN has been discussed theoretically by K. S. Kim, M. G. Cheong, C.-H. Hong, G. M. Yang, K. Y. Lim, E.-K. Suh, and H. J. Lee [*Appl. Phys. Lett.* **76**, 1149 (2000)].

10.12.3 High-Field Transport: Electrons

• **Electron scattering rate**

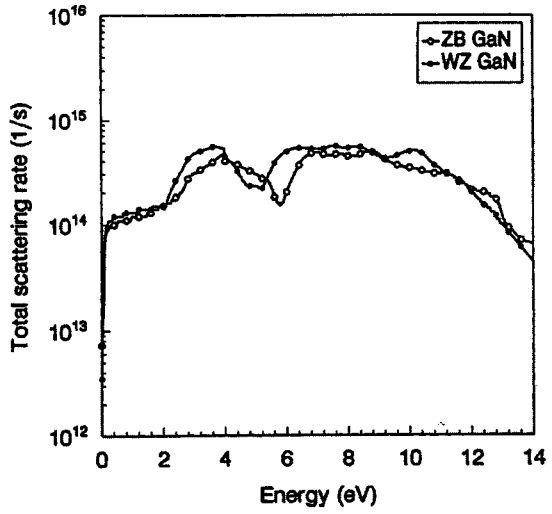

Fig. 10.12.8 Calculated total scattering rate by phonons in α-GaN (WZ) as a function of electron energy, together with that of β-GaN (ZB). [From J. Kolník, I. H. Oğuzman, K. F. Brennan, R. Wang, and P. P. Ruden, *J. Appl. Phys.* **81**, 726 (1997).]

• **Electron drift velocity–field characteristic**

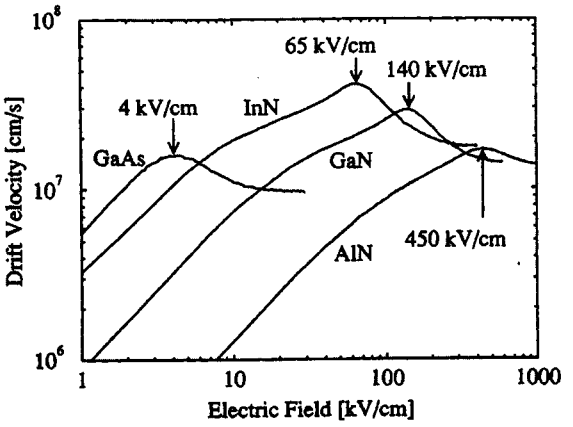

Fig. 10.12.9 Calculated velocity–field characteristic for electrons in α-GaN, together with those for w-AlN, InN, and GaAs (all at 300 K with n=10^{17} cm^{-3}). The arrows indicate the electric fields at which the peak drift velocity is achieved for each velocity–field characteristic. [From B. E. Foutz, S. K. O'Leary, M. S. Shur, and L. F. Eastman, *J. Appl. Phys.* **85**, 7727 (1999).]

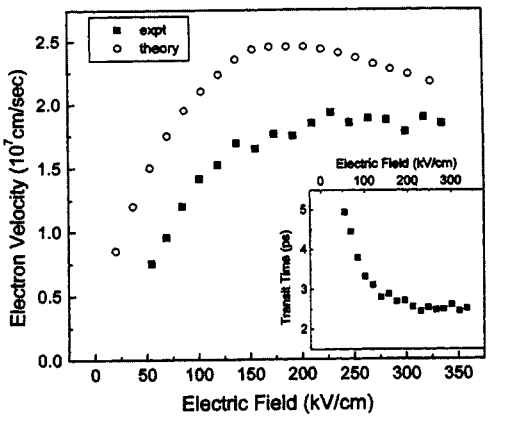

Fig. 10.12.10 Steady-state electron velocity and electron transit time as a function of electric field in α-GaN measured at 300 K. The open circles show the theoretical calculation using a full-zone band structure. [From M. Wraback, H. Shen, J. C. Carrano, T. Li, J. C. Campbell, M. J. Schurman, and I. T. Ferguson, *Appl. Phys. Lett.* **76**, 1155 (2000).]

• **Electron saturation drift velocity**

Table 10.12.3 *Electron saturation drift velocity $v_{e,sat}$ in α-GaN at 300 K [12.4].*

$v_{e,sat}$ (10^7 cm/s)
≤1.9

[12.4] M. Wraback, H. Shen, J. C. Carrano, T. Li, J. C. Campbell, M. J. Schurman, and I. T. Ferguson, *Appl. Phys. Lett.* **76**, 1155 (2000).

10.12.4 High-Field Transport: Holes

• **Hole scattering rate**

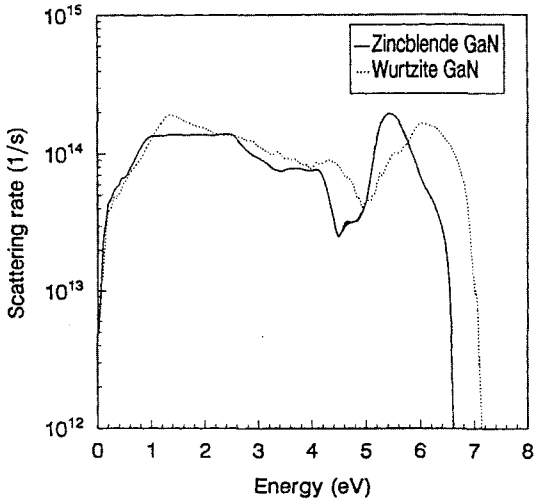

Fig. 10.12.11 Calculated scattering rate of holes in α-GaN (wurtzite) as a function of hole energy, together with that of β-GaN (zincblende). [From I. H. Oğuzman, E. Bellotti, K. F. Brennan, J. Kolník, R. Wang, and P. P. Ruden, *J. Appl. Phys.* **81**, 7827 (1997).]

• **Hole drift velocity–field characteristic**

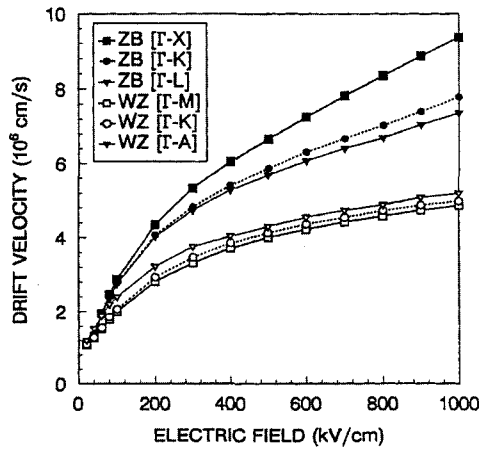

Fig. 10.12.12 Calculated steady-sate hole drift velocity as a function of applied electric field along the three major crystalline axes in α-GaN (WZ), together with that in β-GaN (ZB). [From I. H. Oğuzman, J. Kolník, K. F. Brennan, R. Wang, T.-N. Fang, and P. P. Ruden, *J. Appl. Phys.* **80**, 4429 (1996).]

10.12.5 Minority-Carrier Transport: Electrons in *p*-Type Materials

• **Minority-electron mobility**

Table 10.12.4 *Minority-electron mobility μ in p-type α-GaN at 300 K.*

μ(cm^2/V s)	Comment
0.12	Time-of-flight technique, *p-n* junction UV detector structure [12.5]

[12.5] Z. P. Guan, J. Z. Li, G. Y. Zhang, S. X. Jin, and X. M. Ding, *Semicond. Sci. Technol.* **15**, 51 (2000).

• **Minority-electron lifetime and diffusion length**

Table 10.12.5 *Minority-electron lifetime τ and diffusion length L in p-type α-GaN at 300 K.*

τ (ns)	L (μm)	Comment
0.1	0.20±0.05	MOCVD-grown, dislocation density 5×10^9 cm^{-2} [12.6]

[12.6] Z. Z. Bandić, P. M. Bridger, E. C. Piquette, and T. C. McGill, *Solid-State Electron.* **44**, 221 (2000).

• **Minority-electron diffusion coefficient**

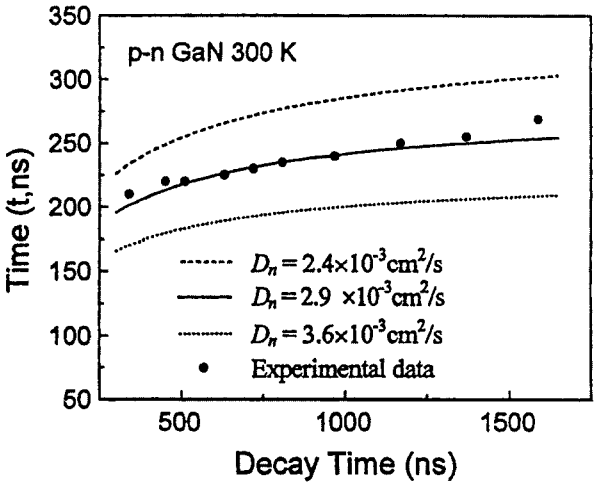

Fig. 10.12.13 Plot of t_{max}, corresponding to maximum current dependence of the lifetime τ (τ_h) of a *p-n* junction GaN UV detector, versus decay time. The minority-electron diffusion coefficient determined from this plot is D_n (D_e)=2.9×10^{-3} cm^2/s. [From Z. P. Guan, J. Z. Li, G. Y. Zhang, S. X. Jin, and X. M. Ding, *Semicond. Sci. Technol.* **15**, 51 (2000).]

10.12.6 Minority-Carrier Transport: Holes in *n*-Type Materials

• **Minority-hole mobility**

Table 10.12.6 *Minority-hole mobility μ in n-type α-GaN at 300 K.*

μ(cm^2/V s)	Comment
5	Estimated from a diffusion length L~0.28 μm and a lifetime τ~6.5 ns [12.7]

[12.7] Z. Z. Bandić, P. M. Bridger, E. C. Piquette, and T. C. McGill, *Appl. Phys. Lett.* **72**, 3166 (1998).

• **Minority-hole lifetime and diffusion length**

Table 10.12.7 *Minority-hole lifetime τ and diffusion length L in n-type α-GaN at 300 K.*

τ (ns)	L (μm)	Comment
	0.1	[12.8]
~15	1.2–3.4	n~5×10^{15}–2×10^{18} cm^{-3} [12.9]
	~1.7–2.5	n~5×10^{17} cm^{-3} [12.10]
≤0.25		Dislocation density (2–5)$\times10^9$ cm^{-2} [12.11]
	1.9	n~3×10^{17} cm^{-3} [12.12]
0.22	0.4	n~7×10^{18} cm^{-3} [12.12]
7	0.28±0.02	n~10^{17} cm^{-3}, dislocation density (2–5)$\times10^9$ cm^{-2} [12.13]
	0.22±0.03	n~10^{16} cm^{-3}, dislocation density 5×10^9 cm^{-2} [12.13]
	1–2	n~10^{16} cm^{-3}, dislocation density 10^8 cm^{-2} [12.13]

[12.8] X. Zhang, P. Kung, D.Walker, J. Piotrowski, A. Rogalski, A. Saxler, and M. Razeghi, *Appl. Phys. Lett.* **67**, 2028 (1995).
[12.9] L. Chernyak, A. Osinsky, H. Temkin, J. W. Yang, Q. Chen, and M. A. Khan, *Appl. Phys. Lett.* **69**, 2531 (1996).
[12.10] J. W. Yang, C. J. Sun, Q. Chen, M. Z. Anwar, M. A. Khan, S. A. Nikishin, G. A. Seryogin, A. V.Osinsky, L. Chernyak, H. Temkin, C. Hu, and S. Mahajan, *Appl. Phys. Lett.* **69**, 3566 (1996).
[12.11] S. J. Rosner, E. C. Carr, M. J. Ludowise, G. Girolami, and H. I. Erikson, *Appl. Phys. Lett.* **70**, 420 (1997).
[12.12] A. Cremades, M. Albrecht, J. Krinke, R. Dimitrov, M. Stutzmann, and H. P. Strunk, *J. Appl. Phys.* **87**, 2357 (2000).
[12.13] Z. Z. Bandić, P. M. Bridger, E. C. Piquette, and T. C. McGill, *Solid-State Electron.* **44**, 221 (2000).

10.12.7 Impact Ionization Coefficient

• Electric-field dependence

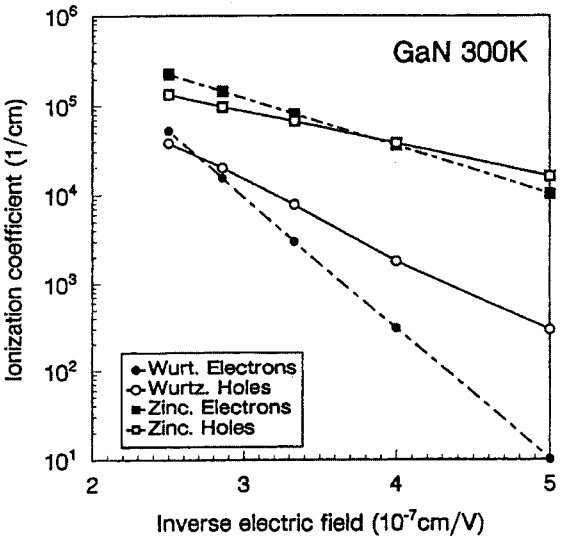

Fig. 10.12.14 Impact ionization coefficient as a function of inverse electric field for electrons and holes in wurtzite- and zinc-blende-phase GaN as calculated using an ensemble Monte Carlo method. The calculations for the wurtzite phase were made for an applied electric field along the Γ–M direction, within the basal plane. The calculations for the zinc-blende phase were performed for an applied electric field along the Γ–X direction. [From I. H. Oğuzman, E. Bellotti, K. F. Brennan, J. Kolník, R. Wang, and P. P. Ruden, *J. Appl. Phys.* **81**, 7827 (1997).]

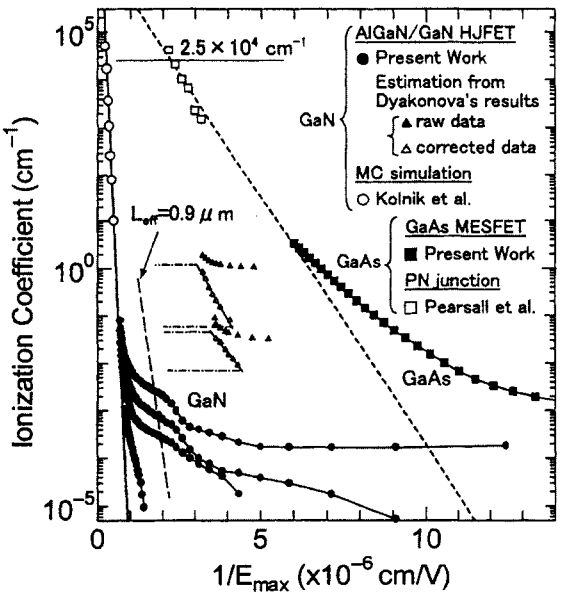

Fig. 10.12.15 Impact ionization coefficient (α) for electrons in GaN extracted from the gate current at V_g=0 V of AlGaN/GaN heterojunction-FETs. The present data are in agreement with Monte Carlo calculation by J. Kolík, I.. H. Oğuzman, K. F. Brennan, R. Wang, and P. P. Ruden [*J. Appl. Phys.* **81**, 726 (1997)]. The line representing L_{eff}=0.9 μm provides the upper bound of α in GaN. The upper bounds of α extracted from the previous work by N. Dyakonova, A. Dickens, M. S. Shur, R. Gaska, and J. W. Yang [*Appl. Phys. Lett.* **72**, 2562 (1998)] are also plotted. For comparison, the results obtained from the gate current of GaAs MESFET's are also plotted. [From K. Kunihiro, K. Kasahara, Y. Takahashi, and Y. Ohno, *IEEE Electron Dev. Lett.* **20**, 608 (1999).]